

# Predicting oscillations in relay feedback systems, using fixed points of Poincaré maps, and Hopf bifurcations

Maben Rabi

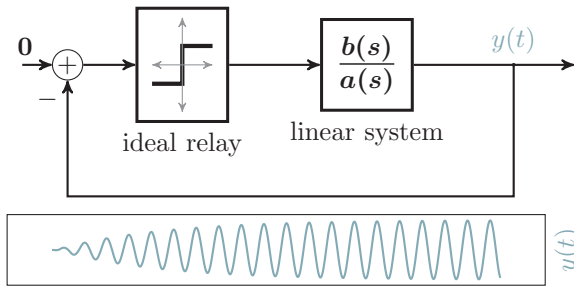


Fig. 1: Spontaneous oscillations under relay feedback.

**Abstract**— The relay autotuning method identifies plant parameters, from oscillations of the plant under relay feedback. To predict the presence and nature of such oscillations, we apply the following two approaches: (a) analysis of the switching dynamics, while using an ideal relay, and (b) bifurcation analysis, while using a smooth approximation of the relay. For stable plants with positive DC gains, our analyses predict that: (i) a periodic orbit is guaranteed, for a class of non-minimum phase plants of relative degree one, whose step response starts with an inverse response, and (ii) for a wider class of plants, whose root locus diagrams cross the imaginary axis at complex conjugate values, limit cycles are merely suggested.

**Index Terms**— Relay feedback, limit cycle, self-oscillations, Relay auto-tuning, Hopf bifurcation, fixed point theorem.

## I. INTRODUCTION

RELAY auto-tuning [1] uses oscillations induced by feedback, to identify a dynamical model for a given plant. The auto-tuner runs a closed-loop experiment, by placing the plant in the Relay feedback system (RFS) shown in Figure 1. If periodic oscillations occur, then the input to the plant is a periodic rectangular wave. Then we can use the period, amplitude and spectrum of the plant’s output, to learn aspects of the plant’s dynamics. For example, suppose that the RFS oscillations are symmetric, and are unimodal meaning that there are exactly two relay switches per period. Then the relay oscillation frequency is a good approximation for some 180-degree phase cross-over frequency of the plant’s transfer function.

A rich variety of dynamical behaviours is possible for relay feedback systems. These include settling into quiescence, asymmetric oscillations [2], chattering [3], and even

chaotic fluctuations [4]–[9]. We do not know yet of broad classes of plants for which oscillations, and their global stability can be guaranteed.

### A. Previous results on relay oscillations

First order plants with positive DC gain, a stable pole, and a time delay have been shown by Åström [10], to self-oscillate. For such a plant, exactly one limit cycle is stable. This is also symmetric, and unimodal. There is an infinity of other periodic orbits, which are all unstable.

Second order plants with a positive DC gain, stable poles, and with one positive zero have been shown to self-oscillate [6], [11]–[13]. The resulting limit cycle is symmetric, unimodal, and globally stable.

Time domain tools such as the Hamel locus [14], [15] and frequency domain tools such as the Tsytkin locus [16] give approximate necessary conditions for limit cycles. But these tools give no direct information about stability. The accuracies of these tools have been discussed, and improved by refinements such as the A-locus variant of the Tsytkin locus, and higher order Describing functions [17]–[24]. Judd [25] concludes that the Tsytkin locus gives more accurate predictions for plant transfer functions with fast roll-off at high frequencies, and that the Hamel locus gives more accurate predictions with slow roll-off.

The classic study of Andronov, Vitt and Khaikin [26], [27] gave a method for analyzing individual second order systems, based on properties of ordinary differential equations on the plane. They proved the stability of some second order valve oscillators, which were significant at that time for Radio engineering.

A state space necessary condition for a symmetrical, periodic orbit is given in Åström [10]. This paper also gives a linearized analysis for local stability in the neighbourhood of a limit cycle. Goncalves et al. [28] show how a Lyapunov analysis for global stability can be carried out. A bifurcation analysis of the RFS, with a plant parameter being the bifurcation parameter is shown in [11], [29].

Megretski [30] gives a graphical template for the step response of a plant, for it to self-oscillate under relay feedback. This template is shown in Figure 2. It shows a positive DC gain, is stable, and has an initial undershoot. Megretski proves that if a given plant step response resembles this template, then self-oscillations are guaranteed, provided that a unique stationary solution exists, for a discrete time iteration involving inter-switching times.

submitted: 2023

Faculty of Computer Sciences, Engineering and Economics, Østfold University College, Halden, Norway (e-mail: first-name.lastname@hiof.no).

arXiv:2306.03394v2 [math.OC] 6 Jul 2023

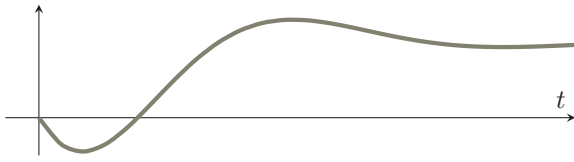


Fig. 2: Megretski’s [30] template for the plant’s open loop step response, to make the closed loop RFS self-oscillate

The map from the state at one switching time to the state after a specified number of switches, has been called the Poincaré map. It has been suggested that RFS limit cycles be studied, by studying fixed points of such maps [31], [32], for example using Banach’s contraction mapping theorem. But only for stable, second order plants has this map been shown to be contracting. Johansson and Rantzer [33] treat the case of a third order plant with no zeroes, and three distinct, real, stable poles. They find conditions under which the said map obeys an ‘area contraction’ property. When the plant is of higher order, we did not know properties required of plants, under which such maps have fixed points, and whether or not these points are globally or at the least, locally attracting.

**B. Our results**

We study the switching dynamics of the RFS, by appealing to the topological and analytical (holomorphic) properties of trajectories of linear ODEs. In specific, we show in Section III that for stable plants, the Poincaré map is not merely continuous, but analytic.

With this, we guarantee a regular periodic orbit, if the plant is stable, is rational, has relative degree of one, has a positive DC gain, and has an odd number of positive real zeros (Section IV). Thus at least when the relative degree of the plant equals one, the RFS has a periodic orbit, if the plant step response matches Megretski’s template.

In Section V we provide a conditional guarantee of global stability. We consider the strong assumption that a Poincaré map is locally Schur stable, everywhere on a bounded, positively invariant set. Under this, we prove that the promised periodic orbit is in fact a symmetric, unimodal and globally asymptotically stable limit cycle.

We change tools in Section VI. We approximate the relay by a cascade combination of a linear amplifier with high gain, and the hyperbolic tangent function. We take the resulting family of smooth nonlinear ODEs, and look for bifurcations and structural stability.

This suggests but does not confirm the presence or absence of limit cycles. We apply the Hopf bifurcation theorem for systems in Lure feedback form [23], [34]–[36], but also a stronger version due to Alexander and Yorke [37]. These suggest that the number of limit cycles depends on the number of crossings of the imaginary axis, in the root locus diagram of the plant.

Sections VI-F and VI-G present the linearization around periodic orbits for the smooth approximation of the RFS.

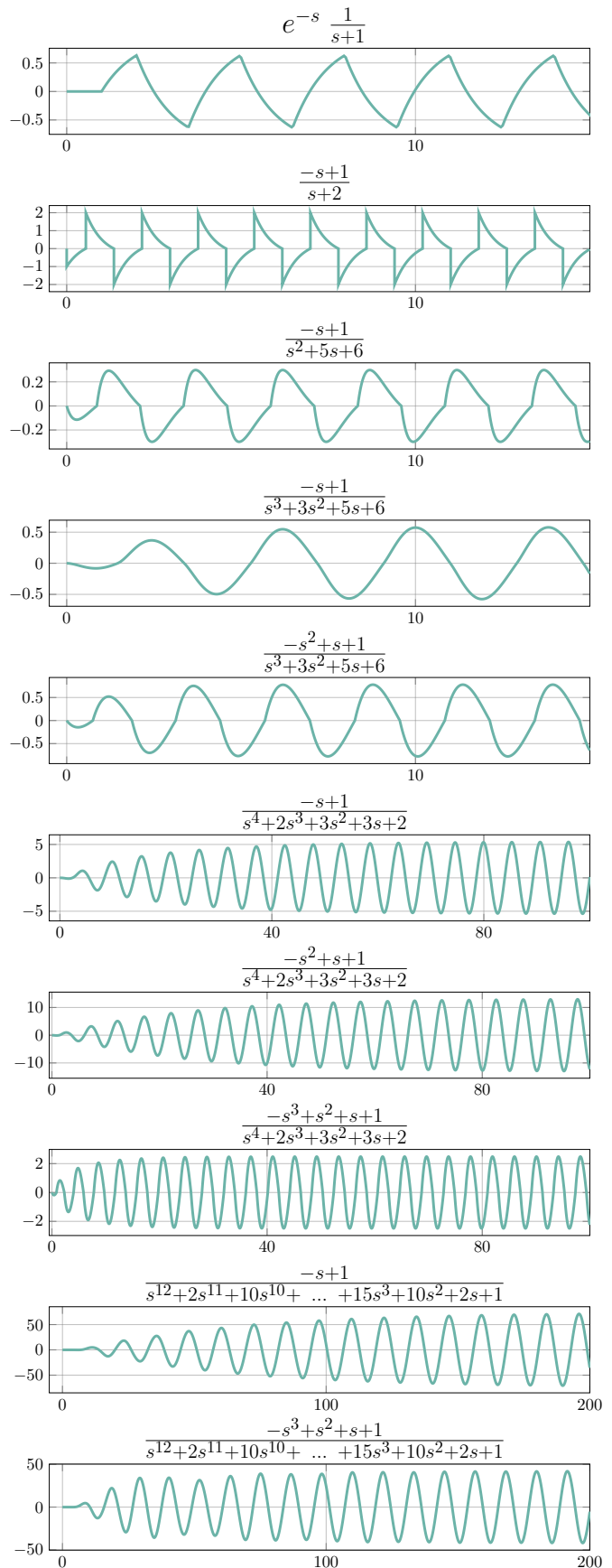


Fig. 3: RFS output for some nonminimum phase plants.

Here our calculations of local stability refine those in [38]–[40]. We end up with an exact expression for the monodromy matrix, which improves that given in [39], when the plant’s relative degree equals one.

## II. PRELIMINARIES

We model the RFS dynamics, first as an ODE with a discontinuous right hand side, and then in the next section, as a nonlinear iteration in discrete-time.

### A. Relay characteristic

We model the relay operator as an ideal binary switch, that has no bias, no delay, and no hysteresis. This is described using the hard signum function:

$$\text{sign}(e) = \begin{cases} +1, & \text{if } e > 0, \\ -1, & \text{if } e < 0, \\ [-1, +1], & \text{if } e = 0. \end{cases}$$

### B. The BRL-URF plants

Let the plant transfer function be:

$$\frac{b(s)}{a(s)} = \frac{b_{n-1}s^{n-1} + \dots + b_0}{s^n + a_{n-1}s^{n-1} + \dots + a_0}. \quad (1)$$

**Definition 1.** A transfer function is **Bounded and RestLess Under Relay Feedback (BRL-URF)** if it is rational, strictly proper, has a pole excess of one, is stable, has positive DC gain, and has an odd number of positive real zeroes.

There are constraints on the signs of some of the coefficients of the transfer function (1), if it is BRL-URF. Firstly, Hurwitz stability requires all the denominator coefficients  $a_i$  to be positive, like the denominator’s leading coefficient is. Then the DC gain being positive forces the numerator’s constant term  $b_0$  to be positive as well. And finally, having an odd number of positive real zeros requires the numerator’s leading coefficient to be negative [45], [46], [53].

The name BRL-URF is suitable because, for such plants, the corresponding RFS has:

- only *bounded* trajectories - this is guaranteed by the Hurwitz stability of the plant (Section IV-A), and,
- only *restless* trajectories, meaning that:
  - the RFS has no equilibrium point, because the DC gain is positive, and,
  - the RFS has no chattering point, because: (i) the DC gain is positive, and (ii) the coefficient  $b_{n-1}$  is negative. See Figure 6, and [40].

Strictly speaking, a sliding set exists, where trajectories cannot be considered to be restless. But at every point on it, non-sliding Filippov solutions also exist. On those points where this non-uniqueness is present, we choose to work with the non-sliding solutions, because with the addition of even the smallest amount of noise, trajectories shall get away from the sliding set, and never return to it.

The step response of a BRL-URF plant matches the template of Megretski - it starts with an inverse response, is bounded, and has a positive steady state.

### C. The state space realization

We use the Observer canonical realization:

$$A = \begin{bmatrix} 0 & 0 & \cdots & \cdots & 0 & -a_0 \\ 1 & 0 & \cdots & \cdots & 0 & -a_1 \\ 0 & 1 & 0 & \cdots & 0 & -a_2 \\ \vdots & \vdots & \ddots & \ddots & \vdots & \vdots \\ 0 & 0 & \cdots & 1 & 0 & -a_{n-2} \\ 0 & 0 & \cdots & 0 & 1 & -a_{n-1} \end{bmatrix}, \quad B = \begin{bmatrix} b_0 \\ b_1 \\ b_2 \\ \vdots \\ b_{n-2} \\ b_{n-1} \end{bmatrix}, \quad (2)$$

$$C = [0 \quad 0 \quad 0 \quad \cdots \quad 0 \quad 1].$$

Then the relay feedback system evolves as per:

$$\frac{d}{dt}x = Ax - B \text{sign}(Cx). \quad (3)$$

### D. Definitions of exit times and exit maps

The switching hyperplane  $\mathcal{S}$  is the set where the relay switches sign. For our chosen realization, it is that hyperplane whose points have zero as the  $x_n$  coordinate:

$$\mathcal{S} = \{x \in \mathbb{R}^n : Cx = 0\}.$$

**Definition 2.** The first exit time from positive sign is the nonnegative function:

$$\tau_+ : \mathbb{R}^n \rightarrow \mathbb{R} \text{ such that } \tau_+(\xi) = \inf \{t > 0 : Cx(t) < 0\},$$

where  $\dot{x} = Ax - B$ , and  $x(0) = \xi$ .

**Definition 3.** The first exit map from positive sign is defined at every point for which the trajectory starting there crosses the switching plane in finite time:

$$\psi_+(\cdot; 1) : \mathbb{R}^n \rightarrow \mathbb{R}^n \text{ such that } \psi_+(\xi; 1) = x(\tau_+),$$

where  $\dot{x} = Ax - B$ , and  $x(0) = \xi$ .

Exactly in analogy to  $\tau_+(\cdot)$ ,  $\psi_+(\cdot; 1)$ , we can define the first exit time function  $\tau_-(\cdot)$ , and first exit map  $\psi_-(\cdot; 1)$  from negative sign, where the ODE in operation shall be:  $\dot{x} = Ax + B$ . Then the following identities hold:

$$\tau_-(x) = \tau_+(-x), \quad \text{and,} \quad \psi_-(x; 1) = -\psi_+(-x; 1).$$

**Definition 4.** For positive integers  $k$ , the  $k$ -th exit map from positive sign for the RFS (3) is defined recursively as follows. For  $k \geq 2$ ,

$$\psi_+(x; k) = \psi_+\left(-\psi_+(x; k-1); 1\right). \quad (4)$$

At any point  $x$ , regardless of whether or not a closed orbit passes through it, we shall call any  $k$ th exit map  $\psi_+(\cdot; k)$ , as a Poincaré map.

The discussions so far lead to the following lemmas.

**Lemma 1.** The first exit time  $\tau_+(\cdot)$  is finite everywhere, when the plant is stable, and has a positive DC gain.

**Lemma 2.** The first exit map  $\psi_+(\cdot; 1)$  exists everywhere, when the plant is stable and has a positive DC gain.

In this paper, the adjective *analytic* means *complex analytic*, which is the same as *holomorphic*. A function from  $\mathbb{C}^n$  to  $\mathbb{C}$  is called analytic, if it is analytic separately in each each element of its argument vector. We say that a

map from the real Euclidean space  $\mathbb{R}^n$  to itself is analytic at a point  $x$ , if there is an analytic extension to this map at  $x$ . In other words, when we embed the point  $x$  in the complex vector space  $\mathbb{C}^n$ , there should be an open ball around  $x$  in the complex domain, where the extended map is complex analytic (it has complex-derivatives of all orders at  $x$ , and has a power series expansion that converges everywhere within the open ball).

Where do analytic maps appear in our analysis? The RFS trajectories that we study are not analytic, but are continuous and piecewise analytic functions of time. In specific, the trajectory coordinates are analytic functions of time, between any two successive relay switches. Next we establish that the first exit times and maps are analytic.

### III. THE POINCARÉ MAP IS ANALYTIC

**Lemma 3.** *Suppose that the plant poles are all non-zero, so that the matrix  $A$  is invertible. If at a point  $\xi \in \mathbb{R}^n$ ,*

$$CA^{-1}B + Ce^{A\tau_+(\xi)} (\xi - A^{-1}B) = 0, \quad (5)$$

$$CAe^{A\tau_+(\xi)} (\xi - A^{-1}B) \neq 0, \quad (6)$$

then the function  $\tau_+(\cdot)$  and the map  $\psi_+(\cdot; 1)$  are analytic in a small neighbourhood of  $\xi$ .

*Proof.* Consider the following analytic function of  $\xi, t$ :

$$\text{output}(\xi, t) \triangleq CA^{-1}B + Ce^{At} (\xi - A^{-1}B)$$

Then  $\tau_+(\xi)$  is implicitly defined through the transcendental equation:  $\text{output}(\xi, \tau_+(\xi)) = 0$ . The partial derivative

$$\left. \frac{\partial}{\partial t} \text{output}(\cdot, \cdot) \right|_{\xi, \tau_+(\xi)} = CAe^{A\tau_+(\xi)} (\xi - A^{-1}B).$$

The Implicit function theorem [41] states that, if the above partial derivative is non-zero, then there is an open neighbourhood of  $\xi$ , on which the implicit function  $\tau_+(\cdot)$  exists, and inherits the continuity, differentiability and analyticity properties of the function:  $\text{output}(\cdot, \cdot)$ . Since the map  $\psi_+(\xi; 1)$  is an analytic function of  $\tau_+$ , it too inherits those properties.  $\square$

**Lemma 4.** *For a given initial condition let the trajectory of a constant coefficient affine ODE cross an analytic hypersurface, after a finite duration. If the crossing is transversal, then locally around the initial condition, there is an open ball where the crossing time, and the crossing map are both defined, and are analytic.*

*Proof.* Crossing the hypersurface transversally at any given point, is nothing other than transversally crossing the tangent hyperplane at that point. The implicit function can be then be used, exactly like for Lemma 3.  $\square$

An *inflection point* for a smooth space curve is a point at which the curve crosses its tangent line. Alternatively, it is a point where there is at least one hyperplane that the curve crosses tangentially.

If a second order transfer function has only non zero poles, then there is no inflection point in any trajectory of the corresponding affine ODE. The curvature at points on

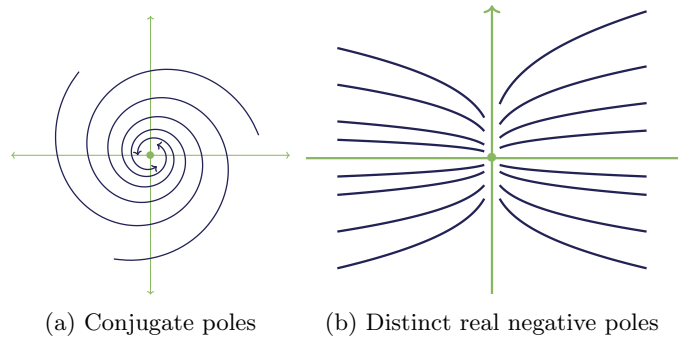


Fig. 4: Trajectories having no inflection points.

any trajectory has the same sign throughout the trajectory, for every trajectory of such an ODE. For example, Figure 4 illustrates the shapes of trajectories for second order plants having stable poles. The following theorem is the equivalent statement for any finite dimension.

**Theorem 1.** *Consider the affine system:*

$$\dot{x} = Ax - B, \quad y = Cx, \quad (7)$$

where the matrix  $A$  and the vectors are given by (2). If  $A$  is stable, then every trajectory that crosses the hyperplane

$$\mathcal{H} \triangleq \{x \in \mathbb{R}^n : Cx = 0\},$$

must cross it transversally.

*Proof.* We shall prove this by contradiction. Assume for the sake of argument, that a trajectory starting at some  $x_0$  crosses the hyperplane tangentially, after a duration of  $\tau$ . If the crossing is indeed tangential, then the crossing point ought to be within at the following set intersection:

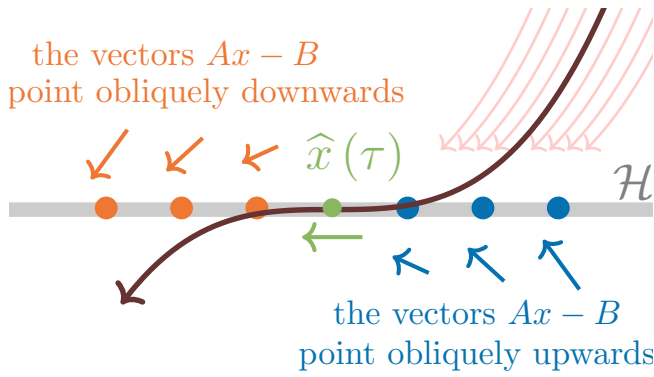
$$\begin{aligned} \mathcal{I} &\triangleq \{x \in \mathbb{R}^n : Cx = 0\} \cap \{x \in \mathbb{R}^n : CAx - CB = 0\}, \\ &= \{x \in \mathbb{R}^n : x_n = 0, \text{ and } x_{n-1} - a_{n-1}x_n - b_{n-1} = 0\}. \end{aligned}$$

Using a topological argument, we shall prove that a crossing via the above set  $\mathcal{I}$  is impossible.

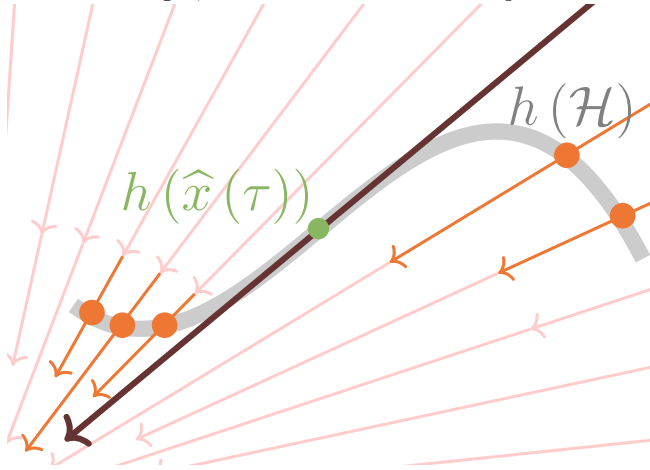
Consider the phase portrait for the observer realization (2), which we have used so far. The two dimensional slice spanned by the coordinates  $x_{n-1}$  and  $x_n$  is shown in Figure 5a. To the left of the hypothetical crossing point, the vector field crosses downwards, in the direction of decreasing  $x_n$ . But to the right, the vector field crosses upwards, in the direction of increasing  $x_n$ .

Arnold (Lemma 3, in § 22, of Chapter 3 from [42]) gives a simpler affine system, that is topologically equivalent (homeomorphic) to the given affine ODE (7). For the ODE (7), consider any positive definite, quadratic Lyapunov function. Level sets of this function are bounded, non-degenerate ellipsoidal shells. Fix such a level set, and call it  $\mathcal{L}$ . Let  $\tau(x)$  denote the finite time it takes for the trajectory starting at a given  $x$  to cross the level set  $\mathcal{L}$ . This crossing must be transversal, since the Lyapunov function is a strictly decreasing function, along any trajectory. With this and Lemma 4, the crossing time  $\tau(x)$  is an analytic function, whenever it is finite. Consider the invertible map:

$$h : x \in \mathbb{R}^n \rightarrow \xi \in \mathbb{R}^n \triangleq e^{-\tau(x)} e^{A\tau(x)} (x - A^{-1}B) + A^{-1}B.$$



(a) The hypothetical trajectory that tangentially crosses the hyperplane  $\mathcal{H}$ ; note that to the left of the hypothetical point of tangential crossing, the vector field crosses  $\mathcal{H}$  downwards, while to the right, the vector field crosses  $\mathcal{H}$  upwards.



(b) The only possible tangential crossing of a smooth hypersurface by a trajectory, for the ODE:  $\frac{d}{dt}\hat{x} = -\hat{x}$ . The vector field crosses downwards the hypersurface  $\tilde{\mathcal{H}}$ , that is  $h(\mathcal{H})$ , on either side of the point of tangential crossing.

Fig. 5: Contradiction between two descriptions of the vector field, around the hypothetical tangential crossing.

Then clearly  $h$  is an analytic diffeomorphism, whenever  $x$  is not equal to the equilibrium point  $A^{-1}B$ .

The flow in the  $\xi$  space is given by the simpler ODE:

$$\frac{d}{dt}\xi = -(\xi - A^{-1}B).$$

Figure 5b depicts the topology of every possible two-dimensional slice, around the mapped crossing point. On either side of the mapped crossing point, the vector field crosses the hypersurface  $\tilde{\mathcal{H}}$  in the same direction, w.r.t. the normal vectors on the hypersurface.

Every analytic diffeomorphism preserves orientedness. The hyperplane  $\mathcal{H}$  separates the two open, half spaces of  $\mathbb{R}^n$ . These must correspond to the two space regions on either side of the analytic hypersurface  $\tilde{\mathcal{H}}$ .

But we have topologically contradictory pictures of the vector fields, around the supposed crossing point. Hence there can be no such tangential crossing point.  $\square$

**Corollary 1.1.** *If a transfer function is rational, proper and*

*stable, then its step response cannot have an inflection point that is also a stationary point.*

**Corollary 1.2.** *If the plant is stable with a positive DC gain, then the corresponding first exit time  $\tau_+(\cdot; 1)$  and first exit map  $\psi_+(\cdot; 1)$  are analytic everywhere on the switching set.*

#### IV. A PERIODIC ORBIT EXISTS

We show that a RFS has a periodic orbit if the plant is BRL-URF, by showing that for sufficiently large number of iterations  $k$ , the map  $-\psi(\cdot; k)$  has a fixed point.

##### A. Bounds on the magnitude of the state

Because the matrix  $A$  is Hurwitz [43]:

$$\|e^{At}\|_2 \leq M_{\text{initial}} e^{-\sigma_{\text{slowest}} t}, \text{ for all nonnegative times } t,$$

where  $M_{\text{initial}}$ ,  $\sigma_{\text{slowest}}$  are positive constants, that depend on the matrix  $A$ . In specific,

$$\sigma_{\text{slowest}} \triangleq \epsilon + \min_{1 \leq i \leq n} |\text{real part of } i\text{th eigenvalue of } A|,$$

where  $\epsilon$  is a positive number that can be arbitrarily small.

Then it follows that the trajectories of the RFS are bounded. In specific, consider an initial state  $x_0 \in \mathbb{R}^n$ . Then at any time  $t$ , we have

$$\begin{aligned} \|x(t)\|_2 &= \left\| e^{At}x_0 + \int_0^t e^{A(t-s)}B \text{sign}(Cx(s)) ds \right\|_2, \\ &\leq \|e^{At}x_0\|_2 + \int_0^t \|e^{A(t-s)}B \text{sign}(Cx(s))\|_2 ds, \\ &\leq M_{\text{initial}} e^{-\sigma_{\text{slowest}} t} \|x_0\|_2 \\ &\quad + M_{\text{initial}} \frac{(1 - e^{-\sigma_{\text{slowest}} t})}{\sigma_{\text{slowest}}} \|B\|_2. \end{aligned} \quad (8)$$

This gives the long-term bound:

$$\lim_{t \rightarrow \infty} \|x(t)\|_2 \leq \frac{M_{\text{initial}}}{\sigma_{\text{slowest}}} \|B\|_2. \quad (9)$$

To bound the state after a finite number of switches, we need bounds on the state that hold after a finite duration of time. Hence we shall use Inequality (8) to derive the looser bounds given in the following two lemmas.

**Lemma 5.** *Let the matrix  $A$  be Hurwitz stable. Let*

$$\tilde{M}_{\text{loose}} \triangleq \mathbf{2} \times \frac{M_{\text{initial}}}{\sigma_{\text{slowest}}} \|B\|_2, \quad (10)$$

*and let the following spherical ball have a radius  $\tilde{M}_{\text{loose}}$ :*

$$\mathcal{B}_{\text{ultimate}} \triangleq \left\{ x \in \mathbb{R}^n : \|x\|_2 \leq \tilde{M}_{\text{loose}} \right\}, \quad (11)$$

*and let the initial state  $x(0)$  lie in the ball  $\mathcal{B}_{\text{ultimate}}$ . For some of the time, the state of the RFS described by Equation (3) could have excursions outside the ball  $\mathcal{B}_{\text{ultimate}}$ . But nevertheless, for all times greater than*

$$t_{\text{excursions-over}} \triangleq \frac{1}{\sigma_{\text{slowest}}} \log(2M_{\text{initial}}), \quad (12)$$

*the state of the RFS is confined to the ball  $\mathcal{B}_{\text{ultimate}}$ .*

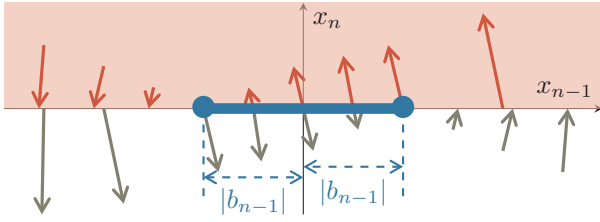


Fig. 6: A slice of the vector fields at switching hyperplane

**Lemma 6.** *Let the matrix  $A$  be Hurwitz stable. If the initial state  $x(0)$  lies in the ball  $\mathcal{B}_{\text{ultimate}}$ , then the subsequent maximum magnitude of the state has the upper bound:*

$$\max_{t \geq 0} \|x(t)\|_2 \leq \widehat{M}_{\text{excursion}} \triangleq \frac{M_{\text{initial}}(2M_{\text{initial}} + 1)}{\sigma_{\text{slowest}}} \|B\|_2. \quad (13)$$

### B. Inter-switch intervals have a positive minimum duration

If the plant is BRL-URF, then the coefficient  $b_{n-1}$  is negative. The set we define next is a subset of the switching set, and it gains special significance:

$$\mathcal{Q} \triangleq \{x \in \mathcal{S} : |x_{n-1}| < |b_{n-1}|\} \quad (14)$$

We call it the *evanescent strip*, because no trajectory from outside the strip lands on it, and the first exit maps take the points on this strip to points on the switching set outside the evanescent strip. As Figure 6 shows, the vector field points away from the strip, under both positive and negative state of the relay. In other words:

- no point on the strip  $\mathcal{Q}$  is in the range of the first exit map from positive sign  $\psi_+(\cdot; 1)$ , and,
- no point on the strip  $\mathcal{Q}$  is in the range of the first exit map from negative sign  $\psi_-(\cdot; 1)$ .

We can construct the sequence of switching points in the trajectory, by alternately applying the maps  $\psi_+(\cdot; 1)$  and  $\psi_-(\cdot; 1)$ . Then, for any arbitrary trajectory, only the starting point could lie in the strip  $\mathcal{Q}$ . No subsequent switching point can lie in the strip.

Therefore, starting from the second interval, over every subsequent inter-switching interval, the trajectory must leap over the strip  $\mathcal{Q}$ . are the times taken by either the affine ODE: Over such an interval of time, the trajectory must travel from a point on the switching set lying on one side of the strip  $\mathcal{Q}$ , to a point on the switching set lying on the opposite side from the strip.

We can then calculate a positive minimum duration for leaping from one side of the strip to the other side, if we restrict the starting point to be from a bounded set.

Consider a trajectory that starts at a point which: (i) is in the ball  $\mathcal{B}_{\text{ultimate}}$ , (ii) also lies on the switching set  $\mathcal{S}$ , and (iii) has its  $(n-1)$ th coordinate greater than  $|b_{n-1}|$ . Since  $b_{n-1}$  is negative, the starting and ending points of the trajectory segment have a mutual distance that is bounded below by the shortest of distances between points on  $\mathcal{S}$  with  $x_{n-1}$  greater than or equal to  $|b_{n-1}|$ , and points

on  $\mathcal{S}$  with  $x_{n-1}$  lesser than or equal to  $-|b_{n-1}|$ . This shortest distance is bounded below by:

$$2|b_{n-1}|.$$

Along any trajectory starting from inside the ball  $\mathcal{B}_{\text{ultimate}}$ , the magnitude of the velocity is bounded above by:

$$\|A\|_2 \widehat{M}_{\text{excursion}} + \|B\|_2.$$

**Lemma 7.** *Consider the RFS described by Equation (3), where the matrices  $A, B, C$  are given by Equation (2). Let the plant be BRL-URF. Let  $\widehat{M}_{\text{loose}}, \mathcal{B}_{\text{ultimate}}, \widehat{M}_{\text{excursion}}$  be defined by Equations (10), (11), and (13) respectively. Then for every trajectory of the RFS that starts from the ball  $\mathcal{B}_{\text{ultimate}}$ , the second and later switching intervals are lower bounded by the following:*

$$t_{\text{minimum-inter-switch}} \triangleq \frac{2|b_{n-1}|}{\|A\|_2 \widehat{M}_{\text{excursion}} + \|B\|_2}. \quad (15)$$

### C. Brouwer's fixed point for the map $-\psi_+(\cdot; k)$

The Brouwer fixed point theorem guarantees a fixed point for a continuous map that takes a closed, bounded and simply connected subset of an Euclidean space to itself. We apply this theorem to the map  $-\psi_+(\cdot; k)$ .

**Lemma 8.** *Consider the RFS (3) for a plant that is BRL-URF. There exists a positive integer  $K$  such that for every integer  $k$  that is greater than or equal to  $K$ , the map*

$$-\psi_+(\cdot; k)$$

*has a fixed point.*

*Proof.* The set we define next lies on the switching set, and is completely on one side of the evanescent strip:

$$\mathcal{D} \triangleq \{x \in \mathcal{S} : x \in \mathcal{B}_{\text{ultimate}}, x \notin \mathcal{Q}, x_{n-1} \geq 0\}. \quad (16)$$

This is the set of points on the switching set that: (i) have lengths less than or equal to  $\widehat{M}_{\text{loose}}$ , (ii) are not on the evanescent strip, and (iii) have a positive value for the  $(n-1)$ th coordinate. In other words, if  $x \in \mathcal{D}$ , then

$$\|x\|_2 \leq \widehat{M}_{\text{loose}}, x_n = 0, \text{ and, } x_{n-1} \geq |b_{n-1}|.$$

For any trajectory that starts from  $\mathcal{D}$ , Lemma 5 implies that the magnitude of switching points is less than or equal to  $\widehat{M}_{\text{loose}}$ , if the number of switches has been at least:

$$K \triangleq \left\lceil \frac{t_{\text{excursions-over}}}{t_{\text{minimum-inter-switch}}} \right\rceil, \quad (17)$$

where the times  $t_{\text{excursions-over}}, t_{\text{minimum-inter-switch}}$  are defined by Equations (12), (15).

Hence if  $k \geq K$ , then

$$x \in \mathcal{D} \implies -\psi_+(x; k) \in \mathcal{D}.$$

Because  $\mathcal{D}$  is bounded and convex, and because the map  $\psi_+(\cdot; k)$  is continuous, the lemma follows from Brouwer's fixed point theorem.  $\square$

**Theorem 2.** *If the plant in the RFS (3) is BRL-URF, then the RFS possesses at least one periodic orbit.*

*Proof.* Pick an integer  $k$  that is greater than or equal to  $K$ . Since  $-\psi_+(\cdot; k)$  has a fixed point in the set  $\mathcal{D}$ , the RFS admits a closed orbit that passes through the set  $\mathcal{D}$ .

The number of distinct switching points that fall within a full traversal of this closed orbit is less than or equal to  $2k$ . We view the orbit as the trajectory that starts at the Brouwer fixed point in the set  $\mathcal{D}$ . Then by Lemma 7, the minimum time interval between two successive switches is at least  $t_{\text{minimum-inter-switch}}$ .

Similarly, the maximum interval between two successive switches can be bounded above. For any trajectory that starts from the set  $\mathcal{D}$ , Lemma 13 guarantees that all subsequent switching points have magnitudes less than or equal to  $\widehat{M}_{\text{excursion}}$ .

Because the plant is BRL-URF, the first exit time  $\tau_+(\cdot)$  is continuous everywhere on the switching plane  $\mathcal{S}$ . Then by the Weierstrass theorem for continuous functions on closed and bounded sets, the function  $\tau_+(\cdot)$  attains its maximum over the following closed and bounded set:

$$\mathcal{S} \cap \left\{ x \in \mathbb{R}^n : \|x\|_2 \leq \widehat{M}_{\text{excursion}}, \text{ and } x_{n-1} \geq |b_{n-1}| \right\}.$$

Therefore the maximum inter-switch time must be finite.

Since the orbit is traversed in finite time, and since it has a finite number of switches, and also because any two successive switches have a positive duration between them, it follows that this is a regular periodic orbit.  $\square$

#### D. Examples of locally stable Poincaré maps

Simple conditions are available for the parameters of possible periodic orbits. The half period  $\tau_+(\widehat{x})$ , and the real vector  $\widehat{x}$  correspond to a symmetric and unimodal periodic orbit, if and only if  $C\widehat{x} = 0$ , and [10]:

$$\begin{cases} C(e^{A\tau_+(x)} + I)^{-1}(e^{A\tau_+(x)} - I)A^{-1}B = 0, \text{ and,} \\ C e^{At}(\widehat{x} - A^{-1}B) + CA^{-1}B \geq 0, \text{ if } 0 \leq t \leq \tau_+(\widehat{x}). \end{cases}$$

For stable second order plants, the first exit map is locally stable, and even contracting [13]. But for higher order plants, we do not know of any guarantees that some Poincaré map is either contracting, or at least locally Schur stable everywhere on some positively invariant set. Numerical experiments indicate that at least for some plants or order three and four, Poincaré maps are locally Schur stable and positively invariant over the set  $\mathcal{D}$ . We first describe the derivatives that we compute numerically.

We have two geometric notions (see Appendix A) of the derivative of the Poincaré map. Both derivatives are calculated by applying the implicit function theorem.

Åström's jacobian [10] has the expression:

$$J_n(x) = \left( I - \frac{1}{Cu}uC \right) e^{A\tau_+(x)}, \quad (18)$$

where the column vector  $u = Ae^{A\tau_+(x)}(x - A^{-1}B)$ , which is the direction of the vector field at the point of crossing the

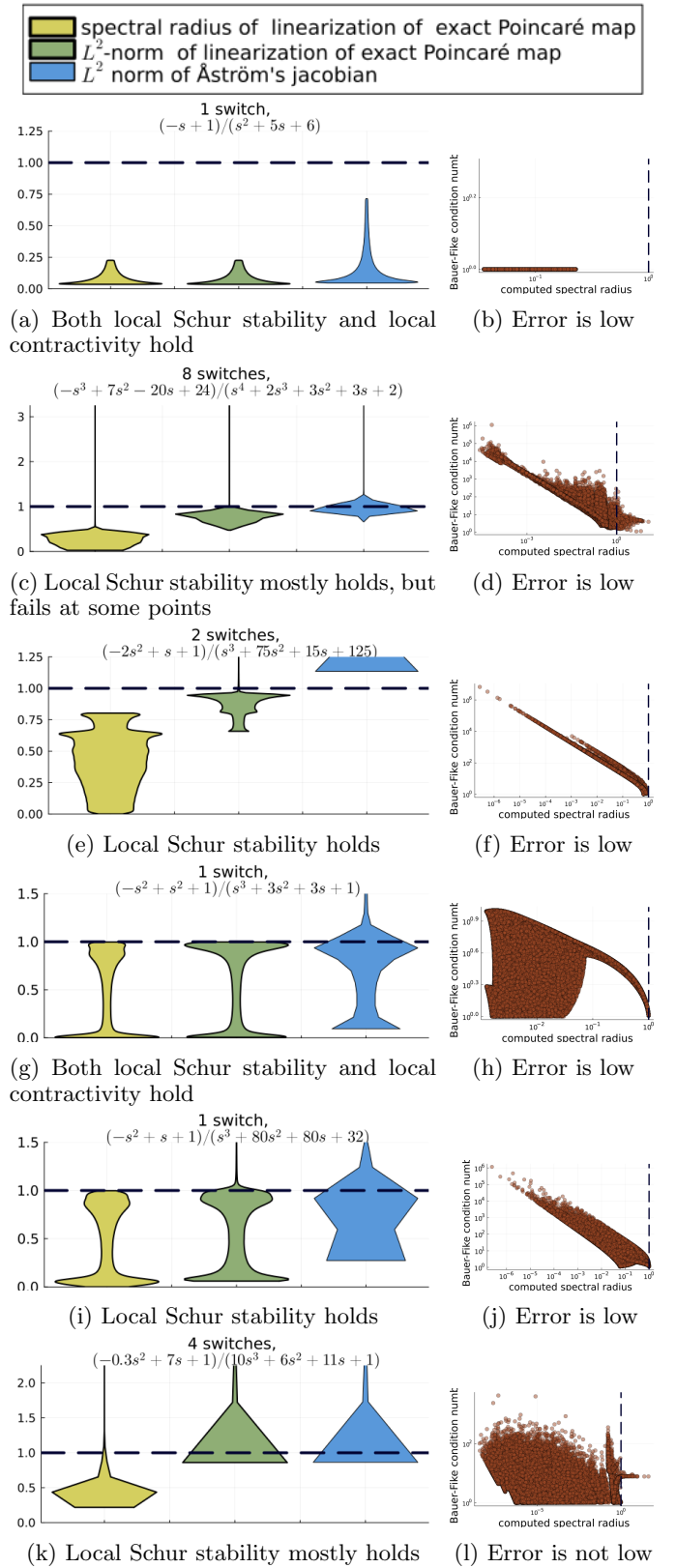


**Fig. 7:** Examples of violin plots of the empirical distribution of spectral radius and  $L^2$  norm, accompanied by scatter plots of the condition numbers - based on a random sample of  $10^6$  points from the set  $\mathcal{D}$ . In these examples, this set happens to be positively invariant for the map  $\psi(\cdot; k)$ , for the given small number  $k$  of iterations (switches).

switching hyperplane, and the row vector  $C$  is the normal to the switching hyperplane, and is given by (2).

The exact derivative of the Poincaré map is:

$$J_{n-1}(x) = \left( I - \frac{1}{Cu} uC \right) e^{A\tau_+(x)} \left( I - \frac{1}{vTv} vv^T \right), \quad (19)$$

where the column vector  $v = A(x - A^{-1}B)$ , which is the direction of the vector field at the starting point  $x$ .

Both derivatives have the same spectral radius (see Appendix A). But the  $L_2$  norm of Åström's jacobian is bigger than or equal to that of the exact jacobian.

For some examples of BRL-URF plants, Figure 7 describes the empirical distributions of the spectral radius, and the  $L_2$  norms of the two jacobians. The sensitivity of a calculated spectral radius is the Bauer-Fike condition number, which is the condition number of the square matrix created by assembling all the eigenvectors.

In our examples, the Bauer-Fike condition number can be high. But for those eigenvalues that are close to or exceed one, the corresponding Bauer-Fike condition numbers are quite low. Hence Schur stability or instability can be concluded with reasonable confidence.

## V. LOCAL STABILITY IMPLIES GLOBAL STABILITY

### A. Why we embed the dynamics in $\mathbb{C}^n$

We cannot generally guarantee global asymptotic stability of a fixed point, even for a smooth map on a bounded Euclidean set that possesses the following two properties: (a) the map meets the requirements of the Brouwer fixed point theorem, and (b) the map has a Schur stable jacobian everywhere. The following example from Shih and Wu [44] illustrates this.

**Example 1** (Schur stable jacobian everywhere does not guarantee global stability of Brouwer's fixed point). Consider the domain  $E \subset \mathbb{R}^2$ , which is defined as the following square shaped set, centered at the origin:

$$\{(x_1, x_2) \in \mathbb{R}^2: |x_1| + |x_2| \leq 1\}.$$

Consider the map  $f : \mathbb{R}^2 \rightarrow \mathbb{R}^2$  defined as follows:

$$f(x_1, x_2) = (\tilde{\mu}(x_2), \tilde{\mu}(x_1)),$$

where,  $\tilde{\mu} : \mathbb{R} \rightarrow \mathbb{R}$  is any function that satisfies:

$$\begin{aligned} \tilde{\mu}(\alpha) &= 0, \text{ if } |\alpha| \leq 1/2, & \tilde{\mu}(1) &= \tilde{\mu}(-1) = 1, \\ |\tilde{\mu}(\alpha)| &\leq 1, \text{ if } |\alpha| \leq 1. \end{aligned}$$

One such smooth map  $\tilde{\mu}$  is the following  $C^4$  function:

$$\tilde{\mu}(\alpha) = \begin{cases} 0, & \text{if } |\alpha| \leq 1/2, \\ 2^5(|\alpha| - 1/2)^5, & \text{if } |\alpha| \geq 1/2. \end{cases}$$

Other alternatives exist for  $\tilde{\mu}$  that are arbitrarily smooth. Regardless of the specific form of  $\tilde{\mu}$ , we have the following:

- Brouwer's fixed point exists, because  $f(E) \subset E$ ,
- the origin is the only fixed point of the function  $f$ ,
- the jacobian at any point  $(x_1, x_2)$  from  $E$  is given by:

$$f_x(x_1, x_2) = \begin{pmatrix} 0 & \tilde{\mu}_{x_2}(x_2) \\ \tilde{\mu}_{x_1}(x_1) & 0 \end{pmatrix}.$$

Both eigenvalues of this matrix are zero !

- But we have at least one cycle of period 1, because:  $f(0, 1) = (1, 0)$  and  $f(1, 0) = (0, 1)$ .

Therefore the origin does not attract all points on  $E$ . Clearly differentiability and Schur stability everywhere on the domain of the map is not sufficient to guarantee the global stability of Brouwer's fixed point. In specific, for the particular  $\tilde{\mu}$  function mentioned above, the origin can only attract those points in the smaller square:  $\{(x_1, x_2) \in \mathbb{R}^2: |x_1| \leq 1/2, \text{ and } |x_2| \leq 1/2\}$ .

We can guarantee the global stability of Brouwer's fixed point, if we have in addition, the holomorphy of the mapping, whose fixed point we are interested in.

### B. Shih-Wu fixed point theorem for bounded, analytic maps

Next comes a theorem that guarantees the global stability of a locally stable fixed point, when Brouwer's fixed point theorem is applied on analytic map acting on a bounded, convex domain. Because we depend on this theorem to study the stability of our RFS limit cycles, we should understand why this result holds. Therefore we repeat below both the theorem and the proof that is given in [44].

**Theorem 3** (the finite-dimensional special case of Theorem 1 from Shih and Wu [44]). Let the domain  $\Delta \subset \mathbb{C}^n$ , and assume that:

- $\Delta$  is non-empty, closed and bounded,
- the interior of  $\Delta$  is an open subset of  $\mathbb{C}^n$ , and
- $\Delta$  is convex.

Let the map  $f : \mathbb{C}^n \rightarrow \mathbb{C}^n$ , and assume that:

- $f$  is analytic on  $\Delta$ ,
- the sequence of iterates of  $f$  is a uniformly bounded sequence of maps, on the domain  $\Delta$ , and,
- there is a fixed point, where the jacobian matrix  $f_z(\cdot)$  is Schur stable.

Then the said fixed point is globally asymptotically stable.

*Proof.* Essentially the proof consists of showing that at least a subsequence of the iterated maps  $f^k$  must converge to a constant map - in specific, the constant map that maps the whole of the domain  $\Delta$  to a single fixed point. We have laid out the proof in the following three steps:

- Step 1: Showing that a locally stable fixed point exists,
- Step 2: Showing that the sequence of iterated maps:  $\{f(\cdot), f^2(\cdot), \dots\}$  has an infinite subsequence that converges to an analytic map, and,
- Step 3: Showing that the sequence of iterated maps:  $\{f(\cdot), f^2(\cdot), \dots\}$  converges to a constant map, which maps the whole of  $\Delta$  to the fixed point.

#### Step 1: Showing that a locally stable fixed point exists

Denote this fixed point by  $\hat{z}$ . Since the jacobian matrix is Schur stable, it follows that there is a small open set  $U$  around the fixed point  $\hat{z}$ , such that for any point in  $U$ , repeated iteration of  $f$  converges to the fixed point  $\hat{z}$ .

#### Step 2: Showing that the sequence of iterated maps: $\{f(\cdot), f^2(\cdot), \dots\}$ has an infinite subsequence that converges to an analytic map

In this step, we use results from Functional analysis that concern the convergence of sequences of maps that are both uniformly bounded and analytic.

Since every map in the sequence  $\{f(\cdot), f^2(\cdot), \dots\}$  takes values inside the bounded set  $\Delta$ , it follows that this sequence is uniformly bounded.

For any bounded domain in  $\mathbb{C}^n$ , the space of continuous mappings from it to itself, is a complete metric space under the supremum norm  $\|\cdot\|_\infty$ . In any complete metric space, every bounded sequence has a convergent subsequence.

Hence it follows that our sequence of iterated maps:  $\{f(\cdot), f^2(\cdot), \dots\}$  has a convergent subsequence. In fact such a subsequence must converge to an analytic limit, as we shall see next.

Any uniformly bounded sequence of analytic maps is uniformly Lipschitz, and therefore *uniformly equicontinuous*<sup>1</sup> (see Theorem 6.1 and Corollary 6.1 of [50]).

By the Arzelà-Ascoli theorem, if a sequence of mappings is uniformly equicontinuous, then it has a subsequence that converges uniformly on every closed and bounded subset of the domain. For us this means that there is an infinite sequence of increasing positive integers:  $\{k_1, k_2, \dots\}$  such that the sequence of iterated mappings:

$$\{f^{k_1}(\cdot), f^{k_2}(\cdot), \dots\}$$

converges uniformly over the set  $\Delta$ .

On an  $n$ -dimensional complex domain<sup>2</sup>, if a sequence of analytic maps is uniformly convergent, then its limit must also be analytic (see [52]). Thus the limit:

$$f_\infty(\cdot) \triangleq \lim_{k_i \rightarrow \infty} f^{k_i}(\cdot),$$

must be analytic on the domain  $\Delta$ .

*Step 3: Showing that the sequence of iterated maps:  $\{f(\cdot), f^2(\cdot), \dots\}$  converges to the constant map that maps every point in  $\Delta$  to the fixed point.*

In this step, we shall use the Identity theorem for analytic mappings, to deduce that the limiting map  $f_\infty$  is constant over the whole of the domain  $\Delta$ .

Recall from Step 1 that the open set  $U$  around the fixed point  $\hat{z}$ , is a basin of attraction for  $\hat{z}$ . Therefore

$$f_\infty(z) \equiv \hat{z} \text{ for every point } z \text{ in the open set } U.$$

Analytic functions behave locally like polynomials. If a polynomial takes a fixed value over a finite interval, then all of its coefficients for positive powers must be necessarily zero. In other words, such a polynomial function must be a constant function. Analytic maps possess a similar property. The identity theorem for several complex variables states that over a  $n$ -dimensional complex domain,

<sup>1</sup>A sequence of mappings is said to be uniformly equicontinuous if for any arbitrary positive number  $\epsilon$ , it is possible to choose a corresponding positive number  $\delta$ , such that every map in the sequence satisfies the following closeness condition: every pair of points that are within a distance of  $\delta$  from each other, is mapped to a pair of image points that are within a distance of  $\epsilon$  from each other.

<sup>2</sup>The equivalent of this statement for Real Euclidean domains is false. The Weierstrass nondifferentiable function [51] is an example of a Fourier series converging uniformly on a finite interval, but to a limit that is continuous but not differentiable.

any analytic function that takes a fixed value over an open subset must be a constant function over the whole domain. This is essentially because constancy over an open subset means that derivatives of all orders are zero, and this reduces the map's power series to the constant term.

Hence it follows that the limit  $f_\infty$  is the constant map:

$$f_\infty(z) \equiv \hat{z}, \text{ for all } z \in \Delta.$$

We shall now show that every infinite subsequence of the iterates of  $f$  converges to the above limit. Consider a number  $k_i$  in the sequence  $\{k_1, k_2, \dots\}$ . The larger  $k_i$  is, the more closely the map  $f^{k_i}(\cdot)$  approximates the map  $f_\infty(\cdot)$ . In fact as  $k_i$  goes to infinity, the approximation error, namely  $f^{k_i}(\cdot) - \hat{z}$ , converges to zero, uniformly over the domain  $\Delta$ . Hence for all large enough  $k_i$

$$\begin{aligned} f^{k_i}(z) &\in U, \text{ for all } z \in \Delta, \text{ and,} \\ \implies f^{k_i+k}(z) &\in U, \text{ for every } k > 0, \end{aligned}$$

which is to say that starting from large enough  $k_i$  all further iterates of  $f$  must also stay inside the open set  $U$ , and converge to the fixed point  $\hat{z}$ .  $\square$

### C. The Poincaré map has a globally convergent fixed point

**Theorem 4** (global convergence to fixed point of Poincaré map). *Let the closed, bounded and convex set  $\mathcal{D} \subset \mathcal{S} \subset \mathbb{R}^n$  be described by Equation (16). Let the integer  $K$  be as per Equation (17), so that the Poincaré map  $\psi_+(\xi; K)$  takes the set  $\mathcal{D}$  to itself. Suppose that the Poincaré map  $\psi_+(\xi; K)$  is locally Schur stable, everywhere on an open set that has the set  $\mathcal{D}$  in its interior. By this we are merely assuming that the said Poincaré map is locally Schur stable at every point on  $\mathcal{D}$ , and also at those points outside  $\mathcal{D}$  that are within a short prescribed distance from its boundary.*

*Then every point of  $\mathcal{D}$  is taken by repeated iterates of the Poincaré map  $\psi_+(\xi; K)$  to the map's Brouwer fixed point.*

*Proof.* We apply the Shih-Wu fixed point theorem for:

$$f(z) = -\psi(z; K), \tag{20}$$

on a suitable domain  $\Delta$  in  $\mathbb{C}^n$ . For our choice of domain, it shall be easy to prove that the map  $f$  is analytic on the domain. But the bulk of this proof shall be devoted to carefully showing that the map  $f$  takes points on the domain, back inside the domain. By showing that, we shall show that the iterates of  $f$  are uniformly bounded.

*Notational conveniences:* (i) given a complex vector  $z \in \mathbb{C}^n$ , and a set of complex vectors  $X \subset \mathbb{C}^n$ , we denote by  $z+X$  that set of complex vectors in  $\mathbb{C}^n$ , formed by adding  $z$  to members of the set  $X$ , and similarly (ii) given a positive real number  $\alpha$ , and a set of complex vectors  $X \subset \mathbb{C}^n$ , we denote by  $\alpha \cdot X$  that set of complex vectors in  $\mathbb{C}^n$ , formed by scaling  $z$  members of the set  $X$ , by the factor  $\alpha$ , (iii) given a complex vector  $z \in \mathbb{C}^n$  we denote by  $|z|_\infty$  the infinity norm of the vector, which is the largest of the magnitudes of its  $n$  component complex numbers, (iv) given a complex vector  $z \in \mathbb{C}^n$ , and a set of complex vectors  $X \subset \mathbb{C}^n$ , we denote by  $|z - X|$  the infimum of all

infinity norms of complex vectors formed by subtracting from  $z$ , members of the set  $X$ ; similarly,  $|z - X|_\infty$  denotes the infimum of norms of the differences between  $z$  and members of  $X$ , and  $(v)$  for a complex vector  $z \in \mathbb{C}^n$ , we denote by  $\text{Re}\{z\}$  and  $\text{Im}\{z\}$  the two real vectors of the real parts and imaginary parts of  $z$ .

Our choice of  $\Delta$  shall contain the real set  $\mathcal{D}$  in its interior. Let  $\epsilon, \eta$  be two positive real numbers of small magnitude. Consider the bounded domain formed by taking the bounded real set  $\mathcal{D}$  and slightly thickening it along all the real and imaginary axes:

$$\begin{aligned} \tilde{\mathcal{D}} &\triangleq \{x \in \mathbb{R}^n : |\text{Re}\{x\} - \mathcal{D}| \leq \epsilon\}, \\ \Delta &\triangleq \{z \in \mathbb{C}^n : |\text{Im}\{z\} - \tilde{\mathcal{D}}|_\infty \leq \eta\}. \end{aligned}$$

In directions parallel to the imaginary axes, we have thickened up to an infinity norm constraint. Hence the boundary  $\partial\Delta$  has two flat faces perpendicular to each imaginary axis. This is used in Steps 2, 3 below.

The rest of the proof consists of showing that:

Step 1:  $f$  is analytic on  $\Delta$ ,

Step 2:  $f$  maps small Schur ellipsoids around  $x \in \mathcal{D}$  to smaller Schur ellipsoids around  $f(x)$ , and,

Step 3:  $f$  maps even the boundary points of  $\Delta$  into  $\Delta$ .

*Step 1:  $f$  is analytic everywhere on  $\Delta$*  The domain  $\Delta$  inherits from the real set  $\mathcal{D}$  the Brouwer fixed point of  $f$ . We can choose  $\epsilon, \eta$  small enough so that  $f$  is analytic on the set of  $\epsilon$ - and  $\eta$ - sized open balls, around points of the real set  $\mathcal{D}$ . The reason is that the set of singularities of  $f$  is at a non zero distance from the closed set  $\mathcal{D}$ .

We can choose  $\epsilon$  small enough so that the Schur stability of the jacobians  $f_z(x)$  on the set  $\mathcal{D}$  also holds on the set  $\tilde{\mathcal{D}}$ .

*Step 2:  $f$  maps small Schur ellipsoids around  $x \in \mathcal{D}$  to smaller Schur ellipsoids around  $f(x)$*  At every  $x \in \mathcal{D}$ , Schur stability of  $f_z(x)$  implies that a symmetric, positive definite matrix  $V(x)$  exists satisfying the Schur equation:

$$[f_z(x)]^T \cdot V(x) \cdot f_z(x) - V(x) = -I.$$

The sublevel sets of the positive definite quadratic form  $z^H V(x) z$  are ellipsoids. We shall consider the action of the map  $f$  on such ellipsoids, around points  $x \in \mathcal{D}$ . We set the sizes of these ellipsoids so that they graze two parallel flat faces of the boundary  $\partial\Delta$ . One of those faces is the following set of all points in  $\Delta$ , such that the last coordinate has the maximum possible imaginary part:

$$\mathcal{F} \triangleq \{z \in \Delta : \text{Im}\{Cz\} = +\eta\}.$$

At each point  $x \in \mathcal{D}$  define the Schur ellipsoid  $\mathcal{E}_x$ , as:

$$\mathcal{E}_x \triangleq \{z \in \mathbb{C}^n : z^H V(x) z \leq r(x)\},$$

where the positive real number  $r(x)$  is chosen such that  $\max_{z \in \mathcal{E}} \text{Im}\{Cz\} = +\eta$ .

For the complex vector  $\delta z$  from the Schur ellipsoid  $\mathcal{E}_x$ , we have the first order Taylor expansion:

$$f(x + \delta z) = f(x) + f_z(x) \delta z + o(\eta) \delta z.$$

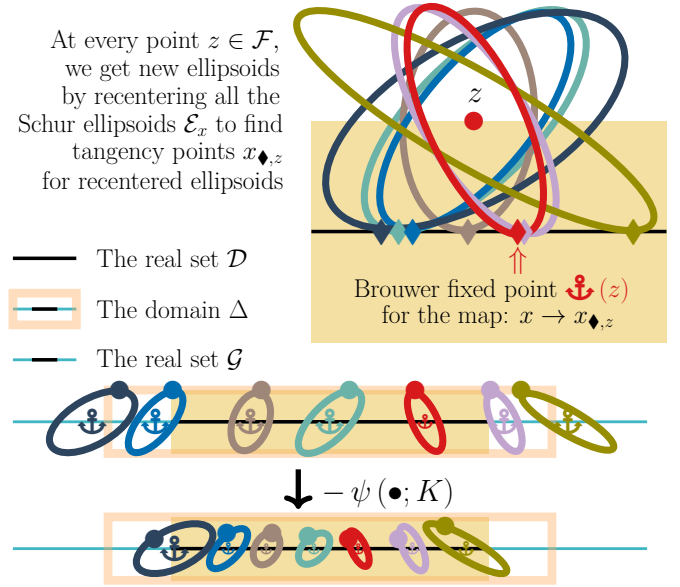


Fig. 8: Schur ellipsoids.

For small enough  $\eta$ , the Schur stability of  $f_z(x)$  implies:

$$f(x + \mathcal{E}_x) \subset f(x) + \frac{\sqrt{\{\sigma_{\max}(V(x))\}^2 - 1}}{\sigma_{\max}(V(x))} \cdot \mathcal{E}_x,$$

where  $\sigma_{\max}(V(x))$  denotes the largest eigenvalue of  $V(x)$ . Thus  $f$  maps the Schur ellipsoid centered at  $x$  to within a shrunken version of the ellipsoid, centered at  $f(x)$ .

*Step 3:  $f$  maps even the boundary points of  $\Delta$  back into  $\Delta$*  The domain  $\Delta$  can be viewed as the set of an infinite collection of sheets that are parallel to the face  $\mathcal{F}$ . Each such sheet is no farther from the set  $\mathcal{D}$  than  $\mathcal{F}$  is.

If a point  $z$  on the face  $\mathcal{F}$  can be included in some Schur ellipsoid centered at some point  $x$  in the real set  $\mathcal{D}$ , then we say that  $z$  is anchored at  $x$ , and we denote that by:

$$x = \mathfrak{A}(z).$$

Since the different Schur ellipsoids have different shapes and orientations, it is not clear whether every point  $z$  on the face  $\mathcal{F}$  can be anchored at a suitable point in  $\mathcal{D}$ .

We need a slightly bigger set, to guarantee such anchoring. Consider the following bounded, convex set

$$\mathcal{G} \triangleq \{x \in \mathbb{R}^n : |x - \tilde{\mathcal{D}}| \leq \epsilon\}.$$

If  $\epsilon$  is small enough, then the jacobian  $f_z(x)$  is Schur stable, everywhere on  $\mathcal{G}$ .

Now consider any point  $z$  on the face  $\mathcal{F}$ . For each point  $x \in \mathcal{G}$ , construct a corresponding Schur ellipsoid  $\mathcal{E}_x$ , but centered at  $z$ . This ellipsoid has a unique point of tangency with the real space  $\mathbb{R}^n$ . Call this point  $x_{\diamond, z}$ .

The map from a point  $x$  to the corresponding tangency point  $x_{\diamond, z}$  is continuous, because  $V(x)$  and  $r(x)$  depend continuously on  $x$ . If  $\eta$  is small enough, then the Schur ellipsoids  $\mathcal{E}_x$  are small, so that every tangency point  $x_{\diamond, z}$  falls within the real set  $\mathcal{G}$ .

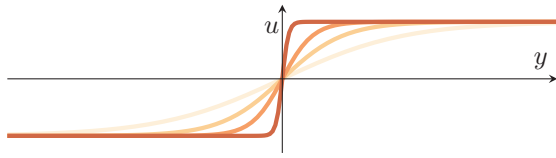


Fig. 9: Ideal relay characteristic asymptotically modelled by the family of smooth functions:  $u = \tanh(\gamma y)$ .

Applying the Brouwer fixed point theorem for the map  $x \rightarrow x_{\diamond, z}$ , on the bounded, convex set  $\mathcal{G}$ , we get at least one fixed point. This fixed point is the anchor for  $z$ .

Since  $f$  maps all points in  $\mathcal{G}$  to within the set  $\mathcal{D}$ , it follows that  $f$  maps all points on  $\mathcal{F}$  to within  $\Delta$ .

For points on the sheets that are parallel to the face  $\mathcal{F}$ , and are closer than  $\mathcal{F}$  to the real set  $\mathcal{D}$ , we can apply the same geometric constructions and arguments as in Steps 2, 3. Then we can conclude that  $f$  maps all points on those sheets to within the domain  $\Delta$ .  $\square$

**Theorem 5.** *If the requirements of Theorem 4 are met, then the RFS (3) has a unique limit cycle that is symmetric, unimodal and globally asymptotically stable.*

*Proof.* Let  $\hat{x} \in \mathcal{D}$  be the Brouwer fixed point for the map  $-\psi_+(\cdot; K)$  promised by Theorem 4. The sequence:

$$\{\hat{x}, -\psi_+(\hat{x}; 1), \dots, -\psi_+(\hat{x}; K-1)\}$$

is a closed cycle for the map  $-\psi_+(\cdot; 1)$ . Every element in this sequence is a fixed point for the map  $-\psi_+(\cdot; K)$ . Therefore, all elements of this sequence have to be the same. Otherwise, we would have a violation Theorem 4.

Hence  $\hat{x}$  is a fixed point for the map  $-\psi_+(\cdot; 1)$ . Hence the RFS has a symmetric, unimodal limit cycle. Every trajectory is ultimately confined to the ball  $\mathcal{B}_{\text{ultimate}}$ , and all trajectories through it must cross the set  $\mathcal{D}$ . Hence the said limit cycle is globally asymptotically stable.  $\square$

## VI. SMOOTH APPROXIMATION OF RELAY ELEMENT

In this section, we do two things: (i) we study a wider class of plant transfer functions than the BRL-URF class, and (ii) we do this by analyzing a smooth approximation of the RFS, by approximating the discontinuous relay operator by the tanh sigmoidal function. We shall vary the approximation parameter for the sigmoid, and as we do that, we look for structural stability of the entire ODE flow, and Hopf bifurcations in which the equilibrium point at the origin produces a limit cycle.

### A. The tanh approximation of the relay element

We shall use the smooth approximation:

$$\text{sign}(y) \approx \tanh(\gamma \cdot y), \quad y \in \mathbb{R},$$

for large enough values of the parameter  $\gamma$ . As shown in Figure 9, the approximation gets better and better for larger and larger choices of the parameter  $\gamma$ . The closed

loop is then the Smooth feedback system (SFS):

$$\frac{d}{dt}\zeta = A\zeta - B \tanh(\gamma C \zeta). \quad (21)$$

where the companion matrix  $A$  and the vectors  $B, C$  are given by Equation (2). The origin is an equilibrium point for this closed loop, at every value of  $\gamma$ . Around this equilibrium point, we get the following linearized flow:

$$\frac{d}{dt}\delta = (A - \gamma BC)\delta. \quad (22)$$

Because the row vector  $C$  has only zero elements except for its last entry, the  $n \times n$  matrix  $BC$  has non-zero elements only on its last column. Therefore the matrix  $A - \gamma BC$  is a companion matrix, whose characteristic polynomial is:

$$\sum_{i=0}^{n-1} (a_i + \gamma b_i) \lambda^i + \lambda^n.$$

### B. Local, global versions of the Hopf bifurcation theorem

By *local bifurcation* we mean a bifurcation (change in the qualitative behaviour of orbits) that holds over an infinitesimally small interval of the bifurcation parameter. By a *global bifurcation* we mean one that holds over some nontrivial finite interval, or an infinite interval.

**Theorem 6** (Local version of the Hopf bifurcation theorem in terms of the Describing function [23], [34]). *Consider the nonlinear feedback system in Lure form:*

$$\frac{d}{dt}\chi = A\chi - B \cdot Y(C\chi, \gamma), \quad \text{for } \chi \in \mathbb{R}^n, \quad (23)$$

where  $\gamma$  is a real-valued parameter. Assume that the scalar-valued function  $Y$  is four times continuously differentiable w.r.t. to the state  $\chi$ , and continuously differentiable w.r.t. the parameter  $\gamma$ . Assume that the origin is an equilibrium point for this feedback system, for all the considered values of  $\gamma$ . Let  $G(s)$  denote the transfer function of the linear plant in the feedback system, meaning that  $G(s) = C(sI - A)^{-1}B$ . Let  $\tilde{G}(s)$  denote the open loop transfer function of the combination of plant and linearization of the nonlinear element, meaning that

$$\tilde{G}(s) = G(s) \cdot \frac{\partial}{\partial \{C\chi\}} Y(C\chi, \gamma) \Big|_{C\chi=0}.$$

Suppose that as  $\gamma$  passes the value  $\gamma_0$ , the Nyquist locus of  $\tilde{G}(j\omega)$  passes the Nyquist critical point  $-1$ , at a unique positive frequency  $\omega_0$ . Suppose that the partial derivatives

$$\frac{\partial}{\partial \gamma} \tilde{G}(j\omega) \Big|_{\substack{\gamma=\gamma_0 \\ \omega=\omega_0}}, \quad \frac{\partial}{\partial \omega} \tilde{G}(j\omega) \Big|_{\substack{\gamma=\gamma_0 \\ \omega=\omega_0}}$$

are nonzero, and as complex numbers are not parallel. This would mean that the Nyquist locus of  $\tilde{G}(j\omega)$  has a generic and non-pathological crossing of the Nyquist critical point. Let  $L(\theta, \omega)$  denote the Describing function of the nonlinear element  $Y$ , for harmonics up to the second one. Suppose that for  $\gamma = \gamma_0$ , and as we vary  $\theta$  the locus of the Describing function  $L(\theta, \omega = \omega_0)$  crosses the Nyquist locus of  $\tilde{G}(j\omega)$  at the Nyquist critical point. If this crossing is transversal,

then a local Hopf bifurcation is guaranteed. In specific, there is a small interval of parameter values that lie on one side of  $\gamma_0$ , such that a limit cycle exists around the equilibrium point. Close to the origin, this limit cycle is unique.

Suppose that the equilibrium point at the origin is stable, before the Hopf bifurcation. If the locus of  $L(\theta, \omega = \omega_0)$  points in a direction outward from the Nyquist locus of  $G(j\omega)$ , then the limit cycle is stable.

We now complement the above local version, with the following global version. The version below requires the same smoothness on the nonlinear element, as the local version above required. The global version predicts the effect of increasing the bifurcation parameter beyond the critical value. It permits only four possible qualitative trends in the subsequent evolution of limit cycle.

**Theorem 7** (Global Hopf bifurcation theorem [37]). Consider the nonlinear feedback system (23). Assume that the nonlinear element in its RHS satisfies the continuous differentiability properties demanded by Theorem 6. Suppose that when  $\gamma = \gamma_0$ , the linearized dynamics at the origin:

$$\frac{d}{dt} \delta = \left( A - BC \cdot \frac{\partial}{\partial \{C\chi\}} Y(C\chi, \gamma) \Big|_{C\chi=0} \right) \delta.$$

has a pair of complex conjugate eigenvalues  $\pm j\omega_0$ . Assume that this eigenvalue has an odd multiplicity.

Assume also that for  $\gamma$  near but not equalling  $\gamma_0$ , the linearization has no eigenvalue with real part zero. Then as  $\gamma$  is increased from the value  $\gamma_0$ , there is at least one periodic orbit that persists in the following sense. The periodic orbit evolves with some non-contradictory combination of the following trends: (T1) a periodic orbit exists for every value of  $\gamma$  that is larger than  $\gamma_0$ , such that the sizes and time periods are both uniformly bounded, and/or (T2) a reverse Hopf bifurcation occurs subsequently, and the family of periodic orbits terminates at an equilibrium point, at some value of  $\gamma$  that is bigger than  $\gamma_0$ , and/or (T3) as the value of  $\gamma$  increases, so does the period of the orbit, and/or (T4) as the value of  $\gamma$  increases, so does the size of the orbit.

We of course care about the first of the above four possible evolution trends for the periodic orbit. Unfortunately, we have found no arguments that could guarantee this trend, and rule out the others.

We shall now apply the above theorems to our SFS (21).

### C. Explanatory power of the plant's root locus diagram

The root locus of the plant shall track the bifurcations undergone by the equilibrium point that the SFS has at the origin. With the examples below, we illustrate the predictive power of the root locus.

Figure 10 shows RFS outputs, for trajectories that start close to the origin. All four plants are stable, and have the same set of poles. But they differ in the sign of the plant zero, and hence in the sign of the DC gain. Explanations of their RFS behaviours are offered by Figure 11.

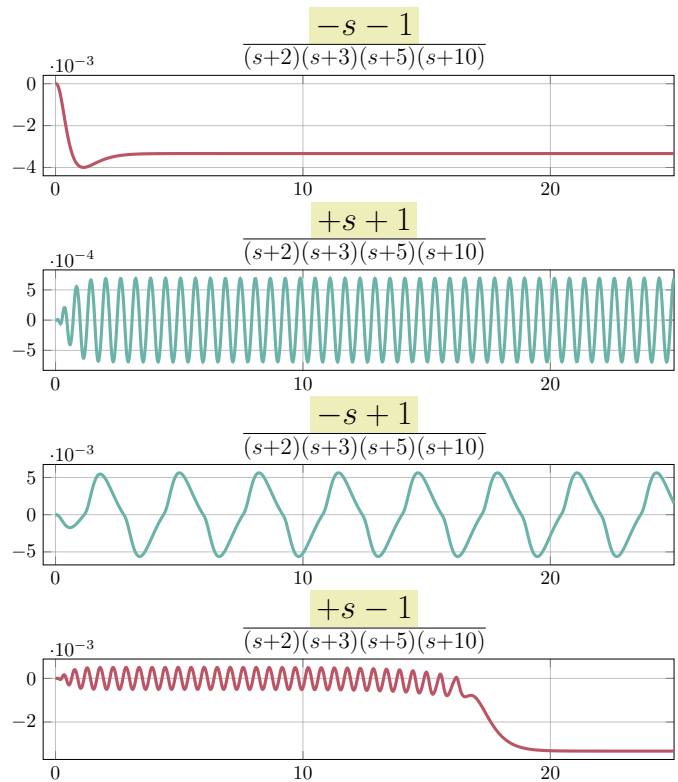


Fig. 10: The sign of plant zero and of the DC gain affect the closed loop behaviour of the RFS.

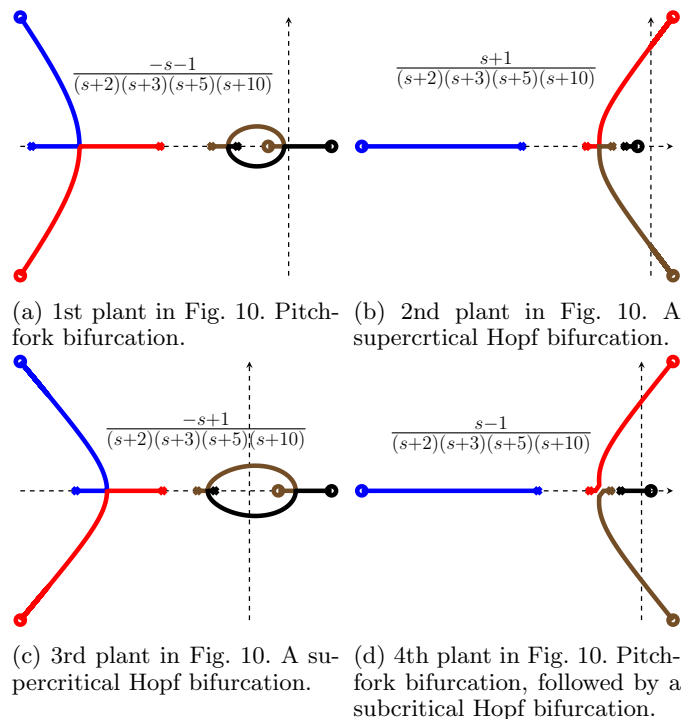


Fig. 11: Explanation for behaviours shown in Figure 10, via the bifurcations predicted by the root loci of the plants.

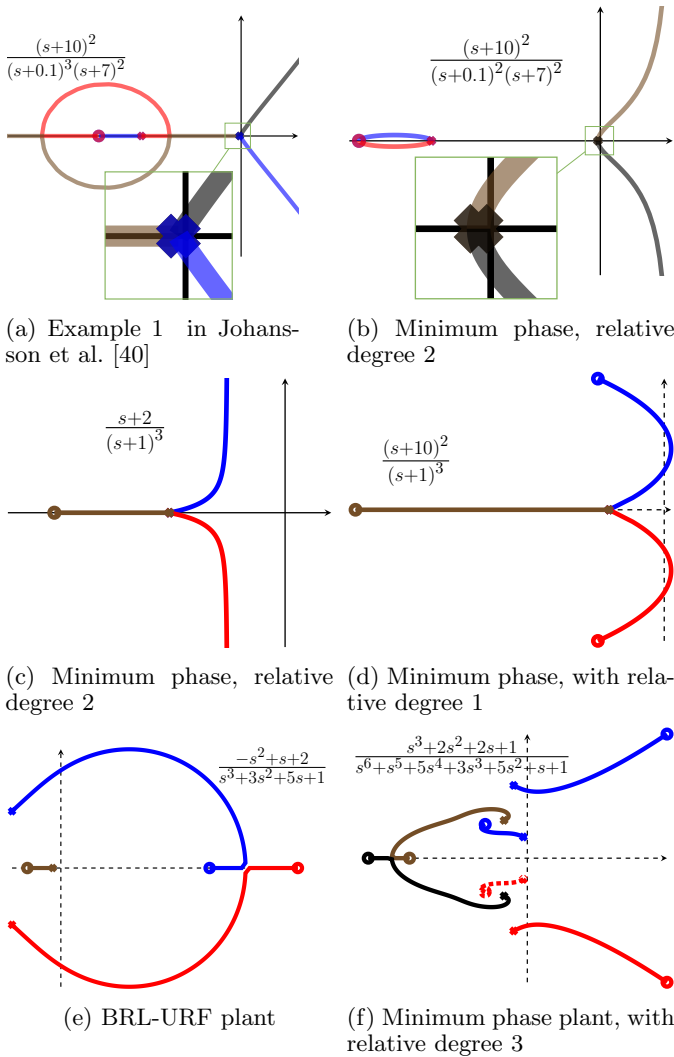


Fig. 12: Example root locus plots for a variety of plants.

In the first plant, a Pitchfork bifurcation produces two stable equilibrium points, and renders the origin unstable. In the second plant, a supercritical Hopf bifurcation produces a stable limit cycle, having a high frequency and a relatively small amplitude. In the third plant, a supercritical Hopf bifurcation produces a stable limit cycle of relatively small frequency. And in the fourth plant, a Pitchfork bifurcation produces two stable equilibrium points, and renders the origin unstable. A subsequent Hopf bifurcation is subcritical.

#### D. RHP zeros, and positive DC gain imply Hopf bifurcations

The SFS shall have Hopf bifurcations, whenever the plant root locus has generic crossings of the imaginary axis, at complex conjugate values. The latter happens, if the plant has a positive DC gain, and RHP zeros.

Two types of zeros, can be associated with any transfer function, as is well known. The transmission zeros come from those finite points in the complex plane where the transfer function vanishes. The ‘zeros at infinity’ come from those close loop poles that grow unboundedly, as the

scalar linear feedback gain is increased to infinity.

Suppose all poles of the open loop plant are stable. If any of either kind of a plant’s zeros are in the RHP, then conditions are ripe for Hopf bifurcations. Every branch of the plant root locus has to start from the LHP. And some branches have to cross over to the RHP; as many branches as there are RHP zeros.

Suppose the plant’s DC gain is positive. Then zero cannot be a closed loop pole, for any value of the negative feedback gain. Hence every cross-over by a root-locus branch must cross the imaginary axis as complex conjugate values. These conditions are sufficient for a local Hopf bifurcation, because of Theorem 6.

The global version due to Theorem 7 also comes into force. We can calculate the Describing function of up to the second harmonic, (see Page 175, [23]) to be:

$$L(\theta, \omega) = -1 + \theta^2 \cdot \frac{\gamma^2}{4} \cdot G(j\omega).$$

At the critical frequency  $\omega_0$ , the locus of  $L_1$  is parallel to the negative real semi-axis. Hence, this locus shall be transversal to, and pointing outwards of the Nyquist locus of  $\tilde{G}(j\omega)$ , unless the latter passes by the point  $-1$  tangentially. Hence generically we can expect that for a stable plant with RHP zeros: (i) as many Hopf bifurcations happen for the SFS, as there are plant root locus crossings of the imaginary axis, and (ii) the first such crossing must give a supercritical Hopf bifurcation.

For a RFS to have a periodic orbit, it is not sufficient that some Describing function analysis predicts it. This can be seen from the example of the root locus diagram in Figure 12d. From this root locus, and the corresponding Nyquist diagram, we see that one periodic orbits is predicted by Describing function analysis. In specific there are two separate transversal intersections of the plant’s Nyquist locus, with the locus of the Describing function that includes up to the second harmonic. The SFS for this plant follows the bifurcation trend (T2), and has a Hopf bifurcation, followed by a reverse Hopf bifurcation.

#### E. SFS for which all trajectories decay towards the origin

For some minimum phase plants having relative degree one or two, we show below that the SFS phase portrait has the same qualitative features, regardless of whether the amplifier gain  $\gamma$  is small or large.

The notion of structural stability concerns the preservation of qualitative features of the behaviour of a dynamical system, under small changes in the governing dynamics.

**Definition 5** (Structural stability). *Consider a dynamical system governed by an ODE. Consider the set of all ODEs obtained by adding to the right hand side of the ODE, perturbations that are both small and continuously differentiable. If for every sufficiently small perturbation, trajectories of the perturbed ODE are topologically equivalent (homeomorphic) to those of the unperturbed ODE, then the dynamical system is said to be structurally stable.*

For any ODE, a *hyperbolic equilibrium point* is one whose linearization has no eigenvalues with real part zero. Locally around any such point, the ODE is structurally stable. This follows from the following two ideas: (i) locally around the hyperbolic equilibrium point, the trajectories of the ODE are homeomorphic to those of the linearization, as per the Hartman-Grobman theorem, and (ii) any small change to the right hand side of the ODE induces continuous changes in the linearization, which in turn induces continuous changes in the eigenvalues.

Similarly, if the jacobian of the right hand side of an ODE is hyperbolic everywhere in a closed and bounded state space, then the ODE is structurally stable. This idea is captured by the notion of Anosov diffeomorphisms and Anosov's guarantee of their structural stability.

**Definition 6** (Anosov diffeomorphism, for Euclidean spaces). *A differential equation of the form:*

$$\frac{dx}{dt} = g(x), \text{ for } x \in X \subset \mathbb{R}^n,$$

*is called an Anosov diffeomorphism over the set  $X$ , if  $X$  is positively invariant under the flow of the ODE, and at every point  $x$  from the set  $X$ , the jacobian matrix*

$$\frac{dg(x)}{dx}$$

*has no eigenvalues with real part zero.*

**Theorem 8** (Theorem 7.9 of [47]). *Anosov diffeomorphisms are structurally stable.*

We now apply these notions to the SFS, for those minimum plants for which no bifurcations can happen, as the parameter  $\gamma$  ranges from 0 to  $+\infty$ .

**Lemma 9.** *If the plant root locus neither crosses nor touches the imaginary axis, then for every nonnegative value of  $\gamma$ , the SFS of Equation (21) is structurally stable.*

*Proof.* We shall show that the jacobian matrix of the RHS of the SFS ODE is hyperbolic, for every nonnegative value of the parameter  $\gamma$ , at every point in the state space.

At any given point  $x$ , the jacobian of the RHS is:

$$A - \frac{\gamma}{\{\cosh(\gamma \cdot Cx)\}^2} BC.$$

We compare this jacobian with that at the origin (Equation (22)), by comparing the functional behaviour of the respective coefficients in front of  $BC$ . For  $\gamma \geq 0$ , we have:

$$\begin{aligned} \frac{\gamma}{\{\cosh(\gamma \cdot Cx)\}^2} &\leq \gamma, \\ \frac{\gamma}{\{\cosh(\gamma \cdot Cx)\}^2} &\leq \frac{0.4478}{|Cx|}, \quad \text{and,} \\ \lim_{\gamma \rightarrow +\infty} \frac{\gamma}{\{\cosh(\gamma \cdot Cx)\}^2} &= \begin{cases} +\infty, & \text{if } Cx = 0, \text{ and,} \\ 0, & \text{if } Cx \neq 0. \end{cases} \end{aligned} \quad (24)$$

By assumption, as  $\gamma$  ranges from 0 to  $+\infty$ , the matrix  $A - \gamma BC$  remains Hurwitz. Hence as  $\gamma/\{\cosh(\gamma \cdot Cx)\}^2$  ranges from 0 to  $0.4478/|Cx|$ , the matrix  $A -$

$(\gamma/\{\cosh(\gamma \cdot Cx)\}^2)BC$  remains Hurwitz. Hence the jacobian is hyperbolic everywhere, for nonnegative values of  $\gamma$ .

A sufficiently large Lyapunov sublevel set for the linear ODE:  $\dot{\chi} = A\chi$ , is positively invariant for the SFS (21), because the extra term involving the tanh function is bounded. Applying Anosov's theorem on this positively invariant set yields the structural stability.  $\square$

The asymptotic behaviour the SFS suggests but does not confirm the asymptotic behaviour of the RFS.

For plants that meet the requirements of the previous lemma, regardless of the nonnegative value of  $\gamma$ , the SFS trajectories decays asymptotically to the origin. If we believe that the behaviour of the RFS is practically indistinguishable from that of the SFS for very high values of  $\gamma$ , then we can also believe that the RFS trajectories move asymptotically in the direction of the origin. If the plant's relative degree is 2, then this suggests that the trajectories decay to the origin. But if the plant's relative degree is 1, then the SFS can only predict the smoothed result of solutions averaged over the sliding portions of the RFS trajectories. Figure 12c gives an example, where the SFS and RFS behaviours seem to coincide empirically.

#### F. Liouville's theorem and local volume shrinkage

For a broad class of periodic orbits that can arise in the SFS (21), we shall now show local volume shrinkage around those orbits, as the gain parameter  $\gamma$  tends to infinity.

Let the SFS (21) possess a periodic orbit of finite period:

$$\{p(t; \gamma) : 0 \leq t \leq T_{\text{period}}\}. \quad (25)$$

Then the linearized flow around this orbit is given by:

$$\frac{d}{dt} \delta = \left[ A - \frac{\gamma}{\{\cosh(\gamma \cdot Cp(t; \gamma))\}^2} BC \right] \delta. \quad (26)$$

Let  $\Phi(t, 0)$  denote the fundamental matrix for the above time-periodic linear system. Differentiating both sides of (21) w.r.t. time, and using the periodicity:

$$\frac{d}{dt} p(t + T_{\text{period}}) = \frac{d}{dt} p(t; \gamma), \quad \text{for all } t \geq 0,$$

we get (Equation 2.6, Chapter 13 of [48]):

$$\Phi(T_{\text{period}}, 0) \frac{d}{dt} p(t; \gamma) = \frac{d}{dt} p(t; \gamma).$$

This means that 1 is an eigenvalue for  $\Phi(T_{\text{period}}, 0)$ .

The product of all eigenvalues can be calculated, by following Willems [49], to give us the following theorem.

**Theorem 9** (local volume shrinkage). *Let the periodic orbit (25) have a finite period. Let the orbit never merely graze without crossing, the hyperplane:  $\{x \in \mathbb{R}^n : Cx = 0\}$ . Let the possible crossings be at isolated time instants, transversal, and finite in number. In other words, if  $Z_p$  denotes the zero set of the signal  $Cp(t; \gamma)$ , then this set must be finite, and transversality means that*

$$C \frac{d}{dt} p(t_0; \gamma) \neq 0, \quad \text{if } t_0 \in Z_p$$

for very large but finite  $\gamma$ , and also in the limit when  $\gamma$  is taken to infinity. Assume that for every time  $t_0 \in Z_p$ , as  $\gamma$  goes to infinity, the signal  $C \frac{d}{dt} p$  has finite left and right limits of the same sign, at all zero crossing times  $t_0$ .

Then as the parameter  $\gamma$  goes to infinity, the determinant of the monodromy matrix  $\Phi(T_{\text{period}}, 0)$  goes to the limit:

$$\exp \left( -a_{n-1} T_{\text{period}} - b_{n-1} \sum_{t_0 \in Z_p} \frac{|\rho^-(t_0)| + |\rho^+(t_0)|}{|\rho^-(t_0) \rho^+(t_0)|} \right),$$

where the left and right limits  $\rho^-(t_0)$ ,  $\rho^+(t_0)$ , are:

$$\begin{aligned} \rho^-(t_0) &\triangleq \lim_{\gamma \rightarrow +\infty} \lim_{\nu \rightarrow 0} C \frac{d}{dt} p(t_0 - |\nu|; \gamma), \text{ and} \\ \rho^+(t_0) &\triangleq \lim_{\gamma \rightarrow +\infty} \lim_{\nu \rightarrow 0} C \frac{d}{dt} p(t_0 + |\nu|; \gamma). \end{aligned}$$

*Proof.* By Liouville's theorem, the determinant of the state transition matrix, namely  $\det(\Phi(t, 0))$ , equals

$$\exp \left( \int_0^t \text{trace} \left( A - \frac{\gamma}{\{\cosh(\gamma \cdot Cp(\hat{t}; \gamma))\}^2} BC \right) d\hat{t} \right).$$

Because the two matrices  $A, C$  have special structure (2),

$$\begin{aligned} &\int_0^t \text{trace} \left( A - \frac{\gamma}{\{\cosh(\gamma \cdot Cp(\hat{t}))\}^2} BC \right) d\hat{t} \\ &= -a_{n-1} t - b_{n-1} \int_0^t \frac{\gamma}{\{\cosh(\gamma \cdot Cp(\hat{t}))\}^2} d\hat{t}. \end{aligned} \quad (27)$$

In the RHS above, the integral multiplying  $b_{n-1}$  can be broken into the following two types of integrals. The first type covers short durations around fast changes of the sigmoidal relay element - these integrals are over infinitesimally small intervals of time, around those instants when the scalar signal  $Cp(t; \gamma)$  crosses zero. And the second type of integrals covers longer durations when there are slight or no changes of the sigmoidal relay element. Thus the integral appearing on the RHS of (27) equals:

$$\begin{aligned} &\sum_{\{t_0 \in Z_p\}} \int_{t_0-\epsilon}^{t_0+\epsilon} \frac{\gamma}{\{\cosh(\gamma \cdot Cp(\hat{t}))\}^2} d\hat{t} \\ &+ \int_{\text{rest of the horizon}} \frac{\gamma}{\{\cosh(\gamma \cdot Cp(\hat{t}))\}^2} d\hat{t}. \end{aligned}$$

As  $\gamma$  goes to infinity, the second integral above goes to zero, in light of (24). In the remaining sum of integrals, each term can be dealt as follows. For finite  $\gamma$  we have:

$$\begin{aligned} \mu_{t_0}(\epsilon; \gamma) &\triangleq \int_{t_0-\epsilon}^{t_0+\epsilon} \frac{\gamma}{\{\cosh(\gamma \cdot Cp(\hat{t}; \gamma))\}^2} d\hat{t}, \\ &= \int_{t_0-\epsilon}^{t_0+\epsilon} \left( \frac{d}{dt} \tanh(\gamma \cdot Cp(\hat{t}; \gamma)) \right) \frac{1}{C \frac{d}{dt} p(\hat{t})} d\hat{t}, \\ &= \int_{t_0-\epsilon}^{t_0} \left( \frac{d}{dt} \tanh(\gamma \cdot Cp(\hat{t}; \gamma)) \right) \frac{1}{C \frac{d}{dt} p(\hat{t})} d\hat{t}, \\ &\quad + \int_{t_0}^{t_0+\epsilon} \left( \frac{d}{dt} \tanh(\gamma \cdot Cp(\hat{t}; \gamma)) \right) \frac{1}{C \frac{d}{dt} p(\hat{t})} d\hat{t}. \end{aligned}$$

We have split the interval of integration into two, because as  $\gamma$  is taken to infinity, in the limit, the signal  $C \frac{d}{dt} p(t)$  is not an analytic function of  $t$ , at  $t = t_0$ . But, even in the limit of  $\gamma$  tending to infinity, this signal is analytic for  $t$  on the semi-open intervals:  $[t_0 - \epsilon, t_0)$ , and  $(t_0, t_0 + \epsilon]$ .

As  $\gamma$  is taken to infinity, the above RHS tends to:

$$\lim_{\epsilon \rightarrow 0} \lim_{\gamma \rightarrow \infty} \mu_{t_0}(\epsilon; \gamma) = \frac{1}{|\rho^-(t_0)|} + \frac{1}{|\rho^+(t_0)|}.$$

Setting  $t = T_{\text{period}}$  in (27) yields the result sought.  $\square$

With this theorem, we cannot conclude outright, the stability of a periodic orbit, except in the case of second order plants. However, we can conclude instability of a periodic orbit, if the determinant of the monodromy matrix is bigger than one. For stable plants, the determinant can exceed one, only if the coefficient  $b_{n-1}$  is negative.

For BRL-URF plants, the coefficient  $b_{n-1}$  is negative. Consider a Hopf bifurcation for the SFS with a BRL-URF plant. Suppose that the critical value of the bifurcation parameter  $\gamma$  is relatively large. Then for values of  $\gamma$  that are only slightly past the critical value, the Hopf limit cycle is still newly born. Hence its amplitude is bound to be infinitesimally small, at these values of  $\gamma$ . Therefore the corresponding output speeds  $\rho^+(t_0), \rho^-(t_0)$ , being proportional to the amplitude, are also bound to be small. On the other hand the period is well approximated by  $2\pi/\omega_0$ , since  $\gamma$  is close to the critical value. Hence, the determinant of the monodromy matrix exceeds one, and the corresponding Hopf limit cycle is unstable at birth.

**Corollary 9.1.** *Let the plant transfer function be proper. Let the sum of its poles be negative, so that the coefficient  $a_{n-1}$  is positive. Let the first nonzero Markov parameter be positive, so that the coefficient  $b_{n-1}$  is either positive, or zero. Now suppose that the SFS (21) possess a periodic orbit (25). Suppose also that this periodic orbit has a finite period, has a finite number of zero crossings, and that such crossings are transversal. Then, as the gain  $\gamma$  is taken to infinity, around this periodic orbit, the linearized flow shrinks volume in phase space.*

### G. The monodromy matrix from the orbit's parameters

Continuing the previous subsection, we illustrate below how to obtain the monodromy matrix  $\Phi(T_{\text{period}}, 0)$ . We shall arrive at this, from knowing the SFS output's speeds at zero crossings, and the orbit's time period. If the plant has a relative degree of two or more, then the SFS output is well approximated by a pure sinusoid, and we shall only need to know the amplitude and time period. We shall calculate the monodromy matrix, by integrating

$$\frac{d}{dt} [e^{-At} \Phi(t, 0)] = \frac{-\gamma}{\{\cosh(\gamma \cdot Cp(t; \gamma))\}^2} BC [e^{-At} \Phi(t, 0)], \quad (28)$$

separately over shorter durations when it changes very fast, and over longer durations when the sigmoidal relay output changes very little, like in the proof of Theorem 9.

Over the second sort of interval, as  $\gamma$  tends to infinity, the RHS of (28) tends to zero, and

$$\Phi(t_2, t_1) \rightarrow e^{A(t_2 - t_1)}.$$

The first sort of interval is infinitesimally small, and so the factor  $e^{-At}$  in the ODE (28) has no effect over the short duration. However there is an effect due to the matrix  $BC$ . This effect describes the change between the tangents to the trajectory, before and after switching.

In the time-varying linear ODE (28), the coefficient matrix at any time commutes with its value at any other time. Hence around any switching time  $t_0$ , we get:

$$\Phi(t_0 + \epsilon, t_0 - \epsilon) = \exp\left(-BC \int_{t_0 - \epsilon}^{t_0 + \epsilon} \frac{\gamma}{\{\cosh(\gamma \cdot Cp(\hat{t}; \gamma))\}^2} d\hat{t}\right), \text{ and}$$

since  $(BC)^k = b_{n-1}^{k-1} BC$ , for  $k \geq 1$ , the above RHS equals

$$I - BC \sum_{k=1}^{\infty} \frac{(-b_{n-1})^{k-1}}{k!} \left( \int_{t_0 - \epsilon}^{t_0 + \epsilon} \frac{\gamma}{\{\cosh(\gamma \cdot Cp(\hat{t}; \gamma))\}^2} d\hat{t} \right)^k$$

If  $b_{n-1}$  is not zero, then the RHS equals:

$$I - BC \frac{1 - \exp\left\{-b_{n-1} \int_{t_0 - \epsilon}^{t_0 + \epsilon} \frac{\gamma}{\{\cosh(\gamma \cdot Cp(\hat{t}; \gamma))\}^2} d\hat{t}\right\}}{b_{n-1}},$$

and if  $b_{n-1}$  equals zero, then the RHS equals

$$I - BC \int_{t_0 - \epsilon}^{t_0 + \epsilon} \frac{\gamma}{\{\cosh(\gamma \cdot Cp(\hat{t}; \gamma))\}^2} d\hat{t}.$$

If  $\gamma$  tends to infinity, then  $\Phi(t_0 + \epsilon, t_0 - \epsilon)$  tends to

$$\begin{cases} I - BC \frac{1 - e^{-b_{n-1} \left( \frac{1}{|\rho^-(t_0)|} + \frac{1}{|\rho^+(t_0)|} \right)}}{b_{n-1}}, & \text{if } b_{n-1} \neq 0, \\ I - BC \left( \frac{1}{|\rho^-(t_0)|} + \frac{1}{|\rho^+(t_0)|} \right), & \text{if } b_{n-1} = 0. \end{cases}$$

The above expression is different from that in Equations 28, 34 in [39]. Those equations were obtained with an arbitrary correction factor. Our derivation is cleaner.

If the plant has a high relative degree, and the periodic orbit in question is symmetric and unimodal, then the output of the SFS as that of the RFS is well approximated by a pure sinusoid. Then the limit:  $1/|\rho^-(t_0)| + 1/|\rho^+(t_0)|$  is well approximated by  $T_{\text{period}}/(\pi M_{\text{peak}})$ , where  $M_{\text{peak}}$  denotes the peak amplitude of the output of the SFS/RFS, for the said periodic orbit. Hence, if the periodic orbit is symmetric and unimodal, then we can use:

$$\Phi(T_{\text{period}}, 0) \approx \left( \left[ I - BC \frac{T_{\text{period}}}{\pi M_{\text{peak}}} \right] e^{AT_{\text{period}}/2} \right)^2.$$

## APPENDIX

### A. TWO JACOBIANS FOR THE POINCARÉ MAP

Consider a switched system, where the state space equals  $\mathbb{R}^n$ , where the dynamics between any two successive switches is affine and time-invariant, and where the switching happens at the crossing of hyperplanes. Consider

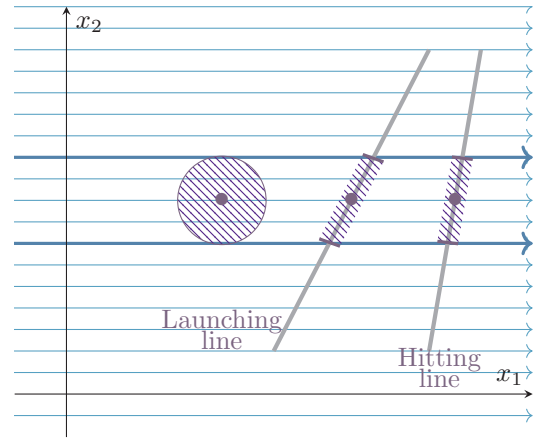


Fig. 13: Example of a Poincaré map whose local stability is not predicted by the spectral radius of  $J_n$ .

two successive switch times. Then we call as the *launching hyperplane* ( $\mathcal{L}$ ) the hyperplane whose crossing was marked by the first time, and we call as the *hitting hyperplane* ( $\mathcal{H}$ ) the hyperplane whose crossing is marked by second time. In the Relay feedback system that we have studied, these two hyperplanes are one and the same. But in general they could be different, and do not even need to be parallel.

Consider a trajectory that starts at  $x \in \mathcal{L}$  and after time  $\tau$ , crosses  $\mathcal{H}$  at the point  $\xi$ . There are two jacobians:

- a matrix of size  $n \times n$  obtained by linearizing the first crossing map for crossing  $\mathcal{H}$ , from an  $n$ -dimensional open ball around  $x$  in  $\mathbb{R}^n$  to an  $n$ -dimensional open ball around  $\xi$ . We call this the unrestricted jacobian, and denote it by the symbol  $J_n$ .
- and a matrix of size  $n - 1 \times n - 1$  obtained by linearizing the first crossing map across  $\mathcal{H}$ , from an  $n - 1$ -dimensional open ball around  $x$  in  $\mathcal{L}$  to an  $n - 1$ -dimensional open ball around  $\xi \in \mathcal{H}$ . We call this the restricted jacobian, and denote it by the symbol  $J_{n-1}$ . Some extra care is needed for calculating this jacobian, because we need to use the same  $n - 1$ -dimensional coordinate system for expressing the vectors in the launching and hitting hyperplanes.

The unrestricted jacobian of the first crossing map from any point  $x$  in the  $\mathbb{R}^n$ -valued state space to the hitting hyperplane can be written (Åström [10]) as a composition of the following two linear transformations: (i) the fundamental matrix of the linearized flow, from time zero to the time of first crossing of the hitting hyperplane, and (ii) the oblique projection onto the hitting hyperplane, along the direction of the vector field at the point of crossing.

In specific, Åström's jacobian is given by Equation (18).

#### A.1 When launching and hitting hyperplanes are not parallel

**Example 2.** Consider the affine flow induced by the following ODE having a constant right hand side:

$$\frac{d}{dt} \begin{pmatrix} x_1 \\ x_2 \end{pmatrix} = \begin{pmatrix} 1 \\ 0 \end{pmatrix}.$$

As shown in Figure 13, the trajectories in phase space are parallel straight lines. Since the coefficient matrix  $A$  is the zero matrix, the exponential  $e^{At}$  is the identity matrix.

Thus, regardless of the orientation of the hitting line, the unrestricted jacobian  $J_n$  is simply equal to the projection along the  $x_1$ -axis onto it. Since the eigenvalues of any projection matrix equal either 0 or 1, it follows that the spectral radius of  $J_n$  is exactly 1.

The restricted jacobian is less than 1, because the Poincaré map is a contraction. The Poincaré map takes line segments in  $\mathcal{L}$  to shorter line segments on  $\mathcal{H}$ .

## A.2 When launching and hitting hyperplanes are parallel

**Lemma 10.** For the  $n \times n$  square matrix  $P$  that represents a linear transformation from  $\mathbb{R}^n$  to itself, assume that:

- The rank of  $P$  is less than or equal to  $n - 1$ .
- $P$  maps the whole of  $\mathbb{R}^n$  to either the whole of, or a subspace of the following linear space:

$$\mathcal{S} \triangleq \{x \in \mathbb{R}^n \mid Cx = 0\},$$

where  $C$  is the following row vector:

$$C = [0 \quad \dots \quad 0 \quad 1].$$

Let us decompose the matrix  $P$  into the following blocks:

$$P = \begin{bmatrix} \underbrace{P_{1:n-1, 1:n-1}}_{n-1} & P_{1:n-1, n} \\ \underbrace{P_{n, 1:n-1}}_n & P_{n, n} \end{bmatrix}.$$

Since  $CPx = 0$  for every  $x \in \mathbb{R}^n$ , it must follow that

$$Px = \begin{pmatrix} P_{1:n-1, 1:n-1} x_{1:n-1} + P_{1:n-1, n} x_n \\ 0 \end{pmatrix}. \quad (29)$$

In other words, both the row vector  $P_{n, 1:n-1}$  and the real number  $P_{n, n}$  must be zeros.

Clearly, the square matrix  $P_{1:n-1, 1:n-1}$  represents a linear transformation from the hyperplane  $\mathcal{S}$  to itself.

Then the matrices  $P$  and  $P_{1:n-1, 1:n-1}$  have the same non-zero eigenvalues, with the same multiplicities.

*Proof.* First we prove that every eigenvalue of  $P_{1:n-1, 1:n-1}$  is an eigenvalue of  $P$ . Suppose  $\lambda$  is an eigenvalue of  $P_{1:n-1, 1:n-1}$  of multiplicity  $k$ . Then there must be exactly  $k$  generalized eigenvectors

$$v_1, \dots, v_k \in \mathbb{C}^{n-1}$$

with possibly complex entries such that for  $0 \leq i \leq k$ :

$$P_{1:n-1, 1:n-1} v_i = \lambda v_i,$$

Thus from Equation 29, it follows that

$$P \begin{pmatrix} v_i \\ 0 \end{pmatrix} = \lambda \begin{pmatrix} v_i \\ 0 \end{pmatrix}, \text{ for } 1 \leq i \leq k.$$

Hence  $\lambda$  is an eigenvalue of  $P$  with a multiplicity of at least  $k$ . Next we prove that  $P$  cannot have a non-zero eigenvalue that is not an eigenvalue of  $P_{1:n-1, 1:n-1}$ .

Suppose for argument's sake that  $\lambda_{\text{extra}}, v_{\text{extra}} \in \mathbb{C}^n$  is an eigenvalue, generalized eigenvector pair for  $P$ , but not for  $P_{1:n-1, 1:n-1}$ . This implies that  $Cv_{\text{extra}} \neq 0$ .

Were  $\lambda_{\text{extra}}$  to be nonzero, then we could write:

$$Cv_{\text{extra}} = \frac{1}{\lambda_{\text{extra}}} CPv_{\text{extra}}.$$

But since  $CPx \equiv 0$  for all  $x \in \mathbb{C}^n$ , it follows that the vector  $v_{\text{extra}}$  could be a generalized eigenvector of  $P$ , only if the corresponding eigenvalue  $\lambda_{\text{extra}}$  is zero.

Since  $P$  can have only one more eigenvalue than  $P_{1:n-1, 1:n-1}$ , it follows that the additional one can only be the zero eigenvalue. Hence the non-zero eigenvalues are in common to both the matrices, and for these eigenvalues the multiplicities are the same.  $\square$

**Corollary 9.2.** For a Poincaré map arising in a switched linear system, assume that the launching and hitting hyperplanes are parallel to each other. Then the restricted and unrestricted jacobians have the same non-zero eigenvalues with the same multiplicities. Therefore both the jacobians have the same spectral radius.

## APPENDIX

### B. RFS OUTPUT BEHAVIOURS FOR SOME PLANTS

The following is a random sample of RFS behaviours. Each entry gives the plant transfer function, its step response, and a short, partial list of RFS behaviours observed.

There is no clearly visible marker in the shape of the plant step response, that could help predict RFS oscillations. What we do notice is that: (1) there seem to be many minimum phase plants whose step responses have an undershoot, and (2) some plants give rise to very spiky trajectories of the RFS.

**TABLE I:** RFS output for plants that are not BRL-URF

Plant	RFS behaviour
-------	---------------

*Known from the previous literature:*

$$\frac{1}{s^2 + \alpha s + \beta},$$

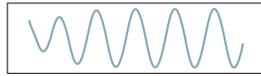
with  $\alpha, \beta > 0$

Origin is globally asymptotically stable [12], [13].



$$\frac{1}{(s + 1)^3},$$

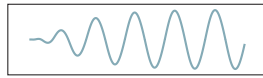
Has a unique symmetric, and unimodal limit cycle - this is locally stable [10]. Trajectories converge to this limit cycle from the origin and from  $[1, 1, 1]^T$



*Simulations of 3rd order plants:*

$$\frac{1}{s^3 + 3s^2 + 5s + 6}$$

Has a symmetric, unimodal limit cycle. Trajectories converge to this limit cycle from the origin, from  $[0.1, 0.1, 0.1]^T$  and from  $[1, 1, 1]^T$ .



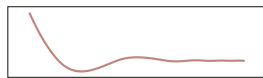
$$\frac{s + 1}{s^3 + 3s^2 + 5s + 6}$$

Trajectories from  $[0.1, 0.1, 0.1]^T$  and from  $[1, 1, 1]^T$  converge to the origin. Trajectory from the origin chatters at the origin.



$\frac{4s + 1}{s^3 + 3s^2 + 5s + 6}$   
 Plant has a zero at  $-0.25$ . This plant has two repeated zeroes at:  $-0.5$ . It is minimum phase. But yet, its step response shows an inverse response, like some minimum phase transfer functions discovered by Maciejowski [53].

Trajectory starting from the origin chatters there. Trajectories from  $[0.01, 0.01, 0.01, 0.01]^T$ , from  $[0.1, 0.1, 0.1, 0.1]^T$ , from  $[1, 1, 1, 1]^T$ , and from  $[10, 10, 10, 10]^T$  settle into the same symmetric, unimodal limit cycle.



Plant	RFS behaviour
-------	---------------

$$\frac{s^2 + s + 1}{s^3 + 3s^2 + 5s + 6}$$

Trajectories starting from the origin, and from  $[1, 1, 1]^T$  chatter on a neighbourhood that is around the origin.

$\frac{s^2 - 2s + 2}{s^3 + 3s^2 + 5s + 6}$   
 Plant has a complex conjugate pair of zeroes on the open RHP.

Trajectories starting from the origin, and from  $[1, 1, 1]^T$  chatter on a neighbourhood that is around the origin.

$\frac{s^2 - 2s + 1}{s^3 + 3s^2 + 5s + 6}$   
 Plant has a real RHP zero at  $+1$ , with multiplicity 2.

Trajectories starting from the origin, and from  $[1, 1, 1]^T$  chatter on a neighbourhood that is around the origin.

$$\frac{s}{s^3 + 3s^2 + 5s + 6}$$

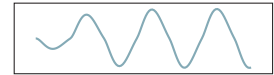
Trajectories starting from the origin, and from  $[1, 1, 1]^T$  chatter on a neighbourhood that is around the origin.

$\frac{s^2 - 2s + 2}{s^3 + 3s^2 + 5s + 6}$   
 Plant has a complex conjugate pair of zeroes on the open RHP.

Trajectories starting from the origin, and from  $[1, 1, 1]^T$  chatter on a neighbourhood that is around the origin.

$\frac{s}{s^3 + 3s^2 + 5s + 6}$   
 Plant has a zero at 0.

Trajectories starting from the origin, and from  $[1, 1, 1]^T$  settle into the same limit cycle.



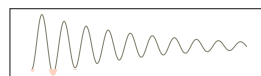
*Simulations of 4th order plants:*

$$\frac{s}{s^3 + 3s^2 + 5s + 6}$$

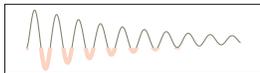
Trajectories starting from the origin, and from  $[1, 1, 1]^T$  chatter on a neighbourhood that is around the origin.

$\frac{s^2 + 2s + 1}{s^4 + 2s^3 + 3s^2 + 3s + 2}$   
 Plant has a complex conjugate pair of zeroes on the open RHP. This plant has two repeated zeroes at:  $-1$ . It is minimum phase. But yet, its step response shows an inverse response, like some minimum phase transfer functions discovered by Maciejowski [53].

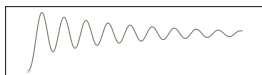
Trajectory starting from the origin chatters there. Trajectories from  $[0.01, 0.01, 0.01, 0.01]^T$ , from  $[0.1, 0.1, 0.1, 0.1]^T$ , from  $[1, 1, 1, 1]^T$ , and from  $[10, 10, 10, 10]^T$  asymptotically reach the origin.



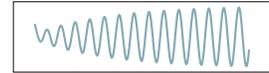
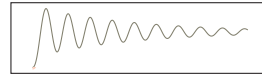
Plant	RFS behaviour
$\frac{(2s + 1)^2}{s^4 + 2s^3 + 3s^2 + 3s + 2}$ Plant has a zero at $-1/2$ , with multiplicity two. This plant has two repeated zeroes at: $-0.5$ . It is minimum phase. But yet, its step response shows an inverse response, like some minimum phase transfer functions discovered by Maciejowski [53].	Trajectory starting from the origin chatters there. Trajectories from $[0.01, 0.01, 0.01, 0.01]^T$ , from $[0.1, 0.1, 0.1, 0.1]^T$ , from $[1, 1, 1, 1]^T$ , and from $[10, 10, 10, 10]^T$ asymptotically reach the origin.



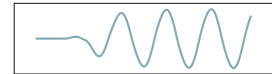
$\frac{(s + 1/4)^2}{s^4 + 2s^3 + 3s^2 + 3s + 2}$ Plant has a zero at $-4$ , with multiplicity two. This plant has two repeated zeroes at: $-0.5$ . It is minimum phase. But yet, its step response shows an inverse response, like some minimum phase transfer functions discovered by Maciejowski [53].	Trajectory starting from the origin chatters there. Trajectories from $[0.01, 0.01, 0.01, 0.01]^T$ , from $[0.1, 0.1, 0.1, 0.1]^T$ , from $[1, 1, 1, 1]^T$ , and from $[10, 10, 10, 10]^T$ settle into the same symmetric, unimodal limit cycle.
--	--



Plant	RFS behaviour
$\frac{s^2 + 5s + 6}{s^4 + 2s^3 + 3s^2 + 3s + 2}$ Plant has a complex conjugate pair of zeroes on the open RHP. This plant has zeroes at: $-2, -3$ . It is minimum phase. But its step response is very oscillatory.	Trajectory starting from the origin chatters there. Trajectories from $[0.01, 0.01, 0.01, 0.01]^T$ , from $[0.1, 0.1, 0.1, 0.1]^T$ , from $[1, 1, 1, 1]^T$ , and from $[10, 10, 10, 10]^T$ reach the same symmetric, unimodal limit cycle.



$\frac{s}{s^3 + 3s^2 + 5s + 6}$ Plant has a zero at 0.	Trajectories starting from the origin, and from $[1, 1, 1]^T$ settle into the same limit cycle.
--	---

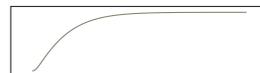


$\frac{s^2 - 0.02s + 0.0001}{s^4 + 2s^3 + 3s^2 + 3s + 2}$	Trajectory starting from $[1, 1, 1]^T$ outputs a series of spikes that decay to zero.
---	---

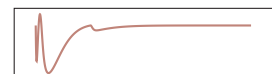
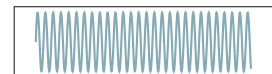


*Simulations of 5th order plants:*

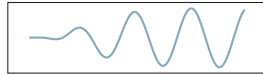
$$\frac{(s + 1)^2}{\{(s + 0.7)^3(s + 7)^2\}}$$



There is a stable symmetric and unimodal limit cycle, that passes through the point:  $[0.2305, 0.4728, 0.2558, 0.0138, 0]^T$ . Trajectory from  $[10, 10, 10, 10, 10]^T$  converges to the origin.



Plant	RFS behaviour
$\frac{s^2 + 5s + 6}{s^5 + 2s^4 + 4s^3 + 4s^2 + 3s + 1}$	Trajectories from the origin, from $[0.1, 0.1, 0.1, 0.1, 0.1, 0.1]^T$ and from $[1, 1, 1, 1, 1, 1]^T$ converge to a symmetric unimodal limit cycle. But Trajectories from $[10, 10, 10, 10, 10, 10]^T$ and from $[50, 50, 50, 50, 50, 50]^T$ converge to a different symmetric unimodal limit cycle.



$\frac{(s + 1)^3}{s^5 + 2s^4 + 4s^3 + 4s^2 + 3s + 1}$	Trajectories from the origin, from $[0.1, 0.1, 0.1, 0.1, 0.1, 0.1]^T$ and from $[1, 1, 1, 1, 1, 1]^T$ converge to a symmetric unimodal limit cycle. But Trajectories from $[10, 10, 10, 10, 10, 10]^T$ and from $[50, 50, 50, 50, 50, 50]^T$ converge to a different symmetric unimodal limit cycle.
---	--



$\frac{(2s + 1)^3}{s^5 + 2s^4 + 4s^3 + 4s^2 + 3s + 1}$	Trajectory from the origin chatters there. Trajectories from $[0.1, 0.1, 0.1, 0.1, 0.1, 0.1]^T$ , from $[1, 1, 1, 1, 1, 1]^T$ , and from $[10, 10, 10, 10, 10, 10]^T$ asymptotically reach the origin. This plant has three repeated zeroes at: $-1$ . It is minimum phase. But yet, its step response shows an inverse response, like some minimum phase transfer functions discovered by Maciejowski [53].
--	--

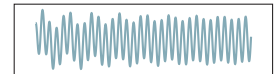


Plant	RFS behaviour
-------	---------------

*Simulations of 6th order plants:*

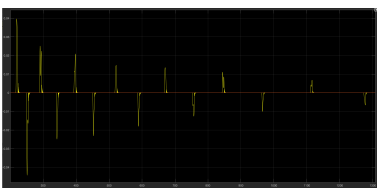
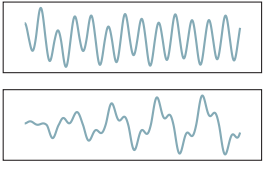
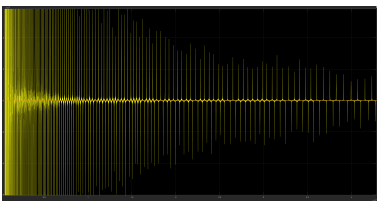
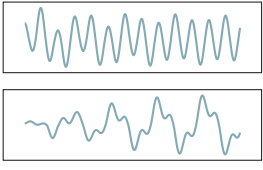
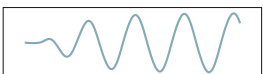
$\frac{s^2}{\left\{ \begin{matrix} s^6 + s^5 + 5s^4 + 3s^3 \\ +5s^2 + s + 1 \end{matrix} \right\}}$	Trajectories from the origin, from $[0.1, 0.1, 0.1, 0.1, 0.1, 0.1]^T$ and from $[1, 1, 1, 1, 1, 1]^T$ and from $[10, 10, 10, 10, 10, 10]^T$ converge to the same symmetric unimodal limit cycle.
---	--

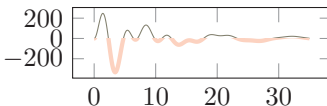
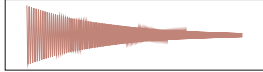
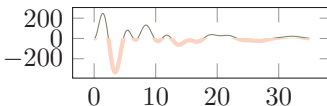
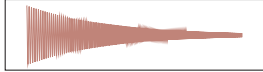
$\frac{s^3}{\left\{ \begin{matrix} s^6 + s^5 + 5s^4 + 3s^3 \\ +5s^2 + s + 1 \end{matrix} \right\}}$	Trajectories from the origin, from $[0.1, 0.1, 0.1, 0.1, 0.1, 0.1]^T$ and from $[1, 1, 1, 1, 1, 1]^T$ converge to a symmetric unimodal limit cycle. But Trajectories from $[10, 10, 10, 10, 10, 10]^T$ and from $[50, 50, 50, 50, 50, 50]^T$ converge to a different symmetric unimodal limit cycle.
---	--

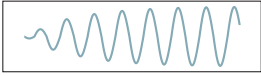


$\frac{s^4}{\left\{ \begin{matrix} s^6 + s^5 + 5s^4 + 3s^3 \\ +5s^2 + s + 1 \end{matrix} \right\}}$	Trajectory from the origin chatters there. Trajectories from $[0.1, 0.1, 0.1, 0.1, 0.1, 0.1]^T$ goes to a symmetric, unimodal limit cycle Trajectories from $[1, 1, 1, 1, 1, 1]^T$ and $[10, 10, 10, 10, 10, 10]^T$ converge to a symmetric limit cycle, which has <i>six switches</i> per period. And trajectories from $[30, 30, 30, 30, 30, 30]^T$ and from $[50, 50, 50, 50, 50, 50]^T$ converge to yet another limit cycle, which is symmetric and unimodal.
---	---

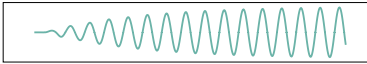


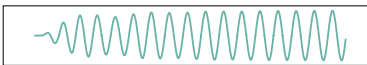
<i>Plant</i>	<i>RFS behaviour</i>	<i>Plant</i>	<i>RFS behaviour</i>
$\frac{-s^5 + s^4 - s^3 - s^2 - s}{\begin{Bmatrix} s^6 + s^5 + 5s^4 + 3s^3 \\ +5s^2 + s + 1 \end{Bmatrix}}$ <p>Plant has an odd number of positive real zeroes at +1, with multiplicity 2.</p>	<p>Trajectories from the origin, from <math>[0.1, 0.1, 0.1]^T</math> and from <math>[1, 1, 1]^T</math> converge to a symmetric unimodal limit cycle. The transient phase is very long, and quasi-periodic.</p> 	$\frac{s^4 - s^3 + s^2}{\begin{Bmatrix} s^6 + s^5 + 5s^4 + 3s^3 \\ +5s^2 + s + 1 \end{Bmatrix}}$	<p>Trajectory starting at the origin chatters there. Trajectories from <math>[0.1, 0.1, 0.1]^T</math> and from <math>[1, 1, 1]^T</math> converge to a symmetric unimodal limit cycle.</p> 
$\frac{s^4 + s^2}{\begin{Bmatrix} s^6 + s^5 + 5s^4 + 3s^3 \\ +5s^2 + s + 1 \end{Bmatrix}}$	<p>Trajectory from <math>[1, 1, 1]^T</math> converges to the origin as a series of decaying spikes. The transient phase is very long.</p> 	$\frac{-s^4 - s^2}{\begin{Bmatrix} s^6 + s^5 + 5s^4 + 3s^3 \\ +5s^2 + s + 1 \end{Bmatrix}}$	<p>Trajectories from the origin, and from <math>[1, 1, 1, 1, 1]^T</math> converge to a symmetric unimodal limit cycle. Trajectories from from <math>[10, 10, 10, 10, 10]^T</math> converge to a different symmetric unimodal limit cycle.</p> 
$\frac{s^4 + s^3 + s^2}{\begin{Bmatrix} s^6 + s^5 + 5s^4 + 3s^3 \\ +5s^2 + s + 1 \end{Bmatrix}}$	<p>Trajectory from <math>[1, 1, 1]^T</math> converges to the origin as a series of decaying spikes. The transient phase is very long.</p> 	$\frac{s^5 + s^4 + s^3 + s^2 + s + 1}{\begin{Bmatrix} s^6 + s^5 + 5s^4 + 3s^3 \\ +5s^2 + s + 1 \end{Bmatrix}}$ <p>This plant has a complex conjugate pair of zeroes on the RHP. These are at: <math>0.5 \pm 0.866\sqrt{-1}</math></p>	<p>Trajectories from reach a chattering set around the origin.</p> 
		$\frac{\begin{Bmatrix} 32s^5 + 16s^4 + 8s^3 \\ +4s^2 + 2s + 1 \end{Bmatrix}}{\begin{Bmatrix} s^6 + s^5 + 5s^4 + 3s^3 \\ +5s^2 + s + 1 \end{Bmatrix}}$ <p>This plant has zeroes that are the zeroes of the previous plant scaled by two. Thus, this plant has a complex conjugate pair of zeroes on at: <math>1 \pm 1.732\sqrt{-1}</math></p>	<p>Trajectory starting from the origin chatters there. Trajectories starting from <math>[0.1, 0.1, 0.1, 0.1, 0.1, 0.1]^T</math>, from <math>[1, 1, 1, 1, 1]^T</math>, and from from <math>[10, 10, 10, 10, 10, 10]^T</math> all converge to the same symmetric unimodal limit cycle.</p> 

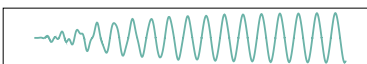
Plant	RFS behaviour	Plant	RFS behaviour
$\frac{s^4 + s^3 + s^2 + s + 1}{\begin{cases} s^6 + s^5 + 5s^4 + 3s^3 \\ +5s^2 + s + 1 \end{cases}}$ <p>This plant has a complex conjugate pair of RHP zeroes at: <math>0.3090 \pm 0.9511\sqrt{-1}</math>.</p>	<p>Trajectory starting from the origin chatters there. Trajectories starting from <math>[0.01, 0.01, 0.01, 0.01, 0.01, 0.01]^T</math>, from <math>[0.1, 0.1, 0.1, 0.1, 0.1, 0.1]^T</math>, and from <math>[1, 1, 1, 1, 1, 1]^T</math> converge to a symmetric, unimodal limit cycle. Trajectory starting from <math>[10, 10, 10, 10, 10, 10]^T</math>, from <math>[20, 20, 20, 20, 20, 20]^T</math>, and from <math>[30, 30, 30, 30, 30, 30]^T</math> all reach another symmetric, unimodal limit cycle.</p>	$\frac{s^4 + 4s^3 + 6s^2 + 4s + 1}{\begin{cases} s^6 + s^5 + 5s^4 + 3s^3 \\ +5s^2 + s + 1 \end{cases}}$ <p>This plant has four repeated zeroes at: <math>-1</math>. It is minimum phase. But yet, its step response shows an inverse response, like some minimum phase transfer functions discovered by Maciejowski [53].</p>	<p>Trajectory starting from the origin chatters there. Trajectories starting from <math>[0.01, 0.01, 0.01, 0.01, 0.01, 0.01]^T</math>, from <math>[0.1, 0.1, 0.1, 0.1, 0.1, 0.1]^T</math>, from <math>[1, 1, 1, 1, 1, 1]^T</math> and from <math>[10, 10, 10, 10, 10, 10]^T</math> converge to a symmetric, unimodal limit cycle.</p>
$\frac{s^3 + s^2 + s + 1}{\begin{cases} s^6 + s^5 + 5s^4 + 3s^3 \\ +5s^2 + s + 1 \end{cases}}$ <p>This plant has no zeroes on the open RHP. It has a conjugate pair of zeroes on the imaginary axis: at <math>\pm\sqrt{-1}</math></p>	<p>Trajectories starting from the origin, from <math>[0.01, 0.01, 0.01, 0.01, 0.01, 0.01]^T</math>, from <math>[0.1, 0.1, 0.1, 0.1, 0.1, 0.1]^T</math>, from <math>[1, 1, 1, 1, 1, 1]^T</math> and from <math>[10, 10, 10, 10, 10, 10]^T</math> converge to a symmetric, unimodal limit cycle.</p>	$\frac{(5s + 1)^4}{\begin{cases} s^6 + s^5 + 5s^4 + 3s^3 \\ +5s^2 + s + 1 \end{cases}}$ <p>This plant has four repeated zeroes at: <math>-0.2</math>. It is minimum phase. But yet, its step response shows an inverse response, like some minimum phase transfer functions discovered by Maciejowski [53]. In fact the step response is ‘exceptionally bad.’</p>	<p>Trajectory starting from the origin chatters there. Trajectories starting from <math>[0.01, 0.01, 0.01, 0.01, 0.01, 0.01]^T</math>, from <math>[0.1, 0.1, 0.1, 0.1, 0.1, 0.1]^T</math>, from <math>[1, 1, 1, 1, 1, 1]^T</math> and from <math>[10, 10, 10, 10, 10, 10]^T</math> reach the origin asymptotically. The transient has high frequency oscillations.</p>
$\frac{s^4 + 2s^3 + 3s^2 + 3s + 2}{\begin{cases} s^6 + s^5 + 5s^4 + 3s^3 \\ +5s^2 + s + 1 \end{cases}}$ <p>This plant has all of its zeroes on the open LHP. It is minimum phase. Its step response is quite oscillatory.</p>	<p>Trajectory starting from the origin chatters there. Trajectories starting from <math>[0.01, 0.01, 0.01, 0.01, 0.01, 0.01]^T</math>, from <math>[0.1, 0.1, 0.1, 0.1, 0.1, 0.1]^T</math>, from <math>[1, 1, 1, 1, 1, 1]^T</math> and from <math>[10, 10, 10, 10, 10, 10]^T</math> converge to a symmetric, unimodal limit cycle.</p>		
			

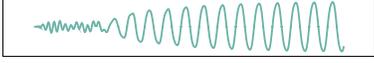
<i>Plant</i>	<i>RFS behaviour</i>
$\frac{-s^5}{\begin{Bmatrix} s^6 + s^5 + 5s^4 + 3s^3 \\ +5s^2 + s + 1 \end{Bmatrix}}$	<p>Trajectories starting from the origin, from <math>[0.1, 0.1, 0.1, 0.1, 0.1, 0.1]^T</math>, from <math>[1, 1, 1, 1, 1, 1]^T</math>, and from <math>[10, 10, 10, 10, 10, 10]^T</math> all reach the same symmetric, unimodal limit cycle.</p> 

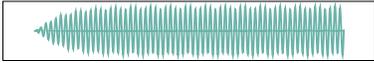
*Simulations of 12th order plants:*

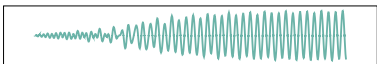
$\frac{-s + 1}{\begin{Bmatrix} s^{12} + 2s^{11} + 10s^{10} \\ +15s^9 + 35s^8 + 37s^7 \\ +53s^6 + 37s^5 + 35s^4 \\ +15s^3 + 10s^2 + 2s + 1 \end{Bmatrix}}$	<p>Trajectory from the origin converges to a symmetric unimodal limit cycle.</p> 
---	--

$\frac{-s^3 + s^2 + s + 1}{\begin{Bmatrix} s^{12} + 2s^{11} + 10s^{10} \\ +15s^9 + 35s^8 + 37s^7 \\ +53s^6 + 37s^5 + 35s^4 \\ +15s^3 + 10s^2 + 2s + 1 \end{Bmatrix}}$	<p>Trajectory from the origin, converges to a symmetric unimodal limit cycle.</p> 
---	---

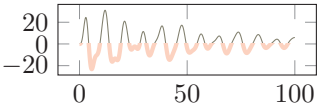
$\frac{\begin{Bmatrix} -s^7 + s^6 \\ +s^5 + s^4 + s^3 \\ +s^2 + s + 1 \end{Bmatrix}}{\begin{Bmatrix} s^{12} + 2s^{11} + 10s^{10} \\ +15s^9 + 35s^8 + 37s^7 \\ +53s^6 + 37s^5 + 35s^4 \\ +15s^3 + 10s^2 + 2s + 1 \end{Bmatrix}}$	<p>Trajectory from the origin, converges to a symmetric unimodal limit cycle.</p> 
---	---

<i>Plant</i>	<i>RFS behaviour</i>
$\frac{\begin{Bmatrix} -s^9 \\ +s^8 + s^7 + s^6 \\ +s^5 + s^4 + s^3 \\ +s^2 + s + 1 \end{Bmatrix}}{\begin{Bmatrix} s^{12} + 2s^{11} + 10s^{10} \\ +15s^9 + 35s^8 + 37s^7 \\ +53s^6 + 37s^5 + 35s^4 \\ +15s^3 + 10s^2 + 2s + 1 \end{Bmatrix}}$	<p>Trajectory from the origin, converges to a symmetric unimodal limit cycle.</p> 

$\frac{\begin{Bmatrix} -s^{10} + s^9 \\ +s^8 + s^7 + s^6 \\ +s^5 + s^4 + s^3 \\ +s^2 + s + 1 \end{Bmatrix}}{\begin{Bmatrix} s^{12} + 2s^{11} + 10s^{10} \\ +15s^9 + 35s^8 + 37s^7 \\ +53s^6 + 37s^5 + 35s^4 \\ +15s^3 + 10s^2 + 2s + 1 \end{Bmatrix}}$	<p>Trajectory from the origin, converges to a symmetric unimodal limit cycle.</p> 
--	---

$\frac{\begin{Bmatrix} -s^{11} + s^{10} + s^9 \\ +s^8 + s^7 + s^6 \\ +s^5 + s^4 + s^3 \\ +s^2 + s + 1 \end{Bmatrix}}{\begin{Bmatrix} s^{12} + 2s^{11} + 10s^{10} \\ +15s^9 + 35s^8 + 37s^7 \\ +53s^6 + 37s^5 + 35s^4 \\ +15s^3 + 10s^2 + 2s + 1 \end{Bmatrix}}$	<p>Trajectory from the origin, converges to a symmetric unimodal limit cycle.</p> 
---	--

This plant is actually BRL-URF. It is listed here for comparison with the previous plants that have the same denominator, but greater pole excess.

Plant	RFS behaviour
$\frac{(s+1)^{10}}{\begin{pmatrix} s^{12} + 2s^{11} + 10s^{10} \\ +15s^9 + 35s^8 + 37s^7 \\ +53s^6 + 37s^5 + 35s^4 \\ +15s^3 + 10s^2 + 2s + 1 \end{pmatrix}}$ <p>This plant has ten repeated zeroes at: <math>-1</math>. It is minimum phase. But yet, its step response shows an inverse response, like some minimum phase transfer functions discovered by Maciejowski [53].</p> 	<p>Trajectory starting from the origin chatters there.</p> <p>Trajectories starting from <math>[0.1, 0.1, 0.1, 0.1, 0.1, 0.1]^T</math>, from <math>[1, 1, 1, 1, 1, 1]^T</math>, and from <math>[10, 10, 10, 10, 10, 10]^T</math> all reach the origin.</p> 

REFERENCES

[1] K. J. Åström and T. Hägglund, “Automatic tuning of simple regulators with specifications on phase and amplitude margins,” *Automatica*, vol. 20, no. 5, pp. 645–651, 1984. [Online]. Available: <https://www.sciencedirect.com/science/article/abs/pii/0005109884900141>

[2] I. Boiko, N. Kuznetsov, R. Mokaev, and E. Akimova, “On asymmetric periodic solutions in relay feedback systems,” *Journal of the Franklin Institute*, vol. 358, no. 1, pp. 363–383, 2021. [Online]. Available: <https://www.sciencedirect.com/science/article/pii/S0016003220307158>

[3] I. Flügge-Lotz, *Discontinuous control systems*. Princeton University press, 1952.

[4] D. V. Anosov, “On stability of equilibrium points of relay systems,” *Automation and Remote control*, vol. 20, no. 2, pp. 135–149, 1959.

[5] P. Cook, “Simple feedback systems with chaotic behaviour,” *Systems & Control Letters*, vol. 6, no. 4, pp. 223 – 227, 1985. [Online]. Available: <http://www.sciencedirect.com/science/article/pii/0167691185900714>

[6] U. Holmberg, “Relay feedback of simple systems,” Ph.D. dissertation, Department of Automatic Control, 1991. [Online]. Available: <https://lucris.lub.lu.se/ws/portalfiles/portal/4722582/8568298.pdf>

[7] K. H. Johansson, A. E. Barabanov, and K. J. Åström, “Limit cycles with chattering in relay feedback systems,” *IEEE Transactions on Automatic Control*, vol. 47, no. 9, pp. 1414–1423, Sep 2002. [Online]. Available: <https://lucris.lub.lu.se/ws/portalfiles/portal/4765935/625671.pdf>

[8] J. Sieber, P. Kowalczyk, S. Hogan, and M. D. Bernardo, “Dynamics of symmetric dynamical systems with delayed switching,” *Journal of Vibration and Control*, vol. 16, no. 7-8, pp. 1111–1140, 2010. [Online]. Available: <https://doi.org/10.1177/1077546309341124>

[9] M. R. Jeffrey, *Hidden dynamics*. Springer, Cham, 2018, the mathematics of switches, decisions and other discontinuous behaviour. [Online]. Available: <https://doi.org/10.1007/978-3-030-02107-8>

[10] K. J. Åström, “Oscillations in systems with relay feedback,” in *Adaptive Control, Filtering, and Signal Processing*, K. J. Åström, G. C. Goodwin, and P. R. Kumar, Eds. New York, NY: Springer New York, 1995, pp. 1–25.

[11] O. A. Chernysheva, “Andronov-Hopf bifurcation theorem for relay systems,” *J. Math. Sci. (N.Y.)*, vol. 200, no. 1, pp. 134–142, 2014, translated from *Sovrem. Mat. Prilozh. No. 85* (2012). [Online]. Available: <https://doi.org/10.1007/s10958-014-1911-2>

[12] M. Rabi, “Relay self-oscillations for second order, stable, non-minimum phase plants,” *IEEE Transactions on Automatic Control*, vol. 66, no. 8, pp. 1–1, 2021.

[13] —, “Relay self-oscillations for second order, stable, nonminimum phase plants,” 2018. [Online]. Available: <https://arxiv.org/abs/1810.11371>

[14] J.-C. Gille, M. J. Pelegrin, and P. Decaulne, *Feedback Control Systems*. MacGraw-Hill book company, Inc., 1959.

[15] J.-F. Le Maitre, J.-G. Paquet, and J.-C. Gille, “A general approach for on-off control systems oscillations,” *Automatica*, vol. 6, no. 4, pp. 609–613, 1970. [Online]. Available: <https://www.sciencedirect.com/science/article/pii/0005109870900154>

[16] Y. Z. Tsytkin, *Relay control systems*. Cambridge: Cambridge University Press, 1984.

[17] E. Bohn, “Stability margins and steady-state oscillations of on-off feedback systems,” *IRE Transactions on Circuit Theory*, vol. 8, no. 2, pp. 127–130, June 1961.

[18] A. Bergen, “A note on Tsytkin’s locus,” *IRE Transactions on Automatic Control*, vol. 7, no. 3, pp. 78–80, April 1962.

[19] H. Weischedel, “An exact method for the analysis of limit cycles in on-off control systems,” *IEEE Transactions on Automatic Control*, vol. 18, no. 1, pp. 40–44, February 1973.

[20] F. F. Judd and P. M. Chirlian, “Graphical analysis and design of limit cycles in autonomous relay control systems,” *International Journal of Control*, vol. 20, no. 2, pp. 321–334, 1974. [Online]. Available: <https://doi.org/10.1080/00207177408932740>

[21] F. F. Judd, “Error bounds for approximate analysis of self-oscillations in autonomous relay control systems,” *International Journal of Control*, vol. 25, no. 4, pp. 557–574, 1977. [Online]. Available: <https://doi.org/10.1080/00207177708922253>

[22] D. Atherton, “Oscillations in relay systems,” *Transactions of the Institute of Measurement and Control*, vol. 3, no. 4, pp. 171–184, 1981. [Online]. Available: <https://doi.org/10.1177/014233128100300401>

[23] A. I. Mees, *Dynamics of Feedback systems*, 1st ed. Chichester: A Wiley-Interscience publication, 1981.

[24] N. Kuznetsov, E. Akimova, R. Mokaev, and M. Morozova, “The study of periodic oscillations and global stability in the Tal’ model via the Tsytkin method and the LPRS method,” *Journal of Physics: Conference Series*, vol. 1864, no. 1, p. 012064, may 2021. [Online]. Available: <https://doi.org/10.1088/1742-6596/1864/1/012064>

[25] F. F. Judd, “Relationships between Tsytkin, Hamel and approximate limit cycle analyses†,” *International Journal of Control*, vol. 21, no. 4, pp. 641–653, 1975. [Online]. Available: <https://doi.org/10.1080/00207177508922018>

[26] A. A. Andronov, A. A. Vitt, and S. E. Khaikin, *Theory of Oscillations*, 2nd ed., ser. International Series of Monographs in Physics, Vol. 4. Oxford: Pergamon press, 1966, Russian edition published as *Teoriya kolebanii*, Moscow: Gostekhizdat, in 1937.

[27] N. Minorsky, *Nonlinear Oscillations*, 1st ed. Van Nostrand, 1962.

[28] J. M. Gonçalves, A. Megretski, and M. A. Dahleh, “Global stability of relay feedback systems,” *IEEE Transactions on Automatic Control*, vol. 46, no. 4, pp. 550–562, Apr 2001.

[29] M. di Bernardo, K. H. Johansson, and F. Vasca, “Self-oscillations and sliding in Relay feedback systems: symmetry and bifurcations,” *International Journal of Bifurcation and Chaos*, vol. 11, no. 04, pp. 1121–1140, 2001. [Online]. Available: <https://doi.org/10.1142/S0218127401002584>

[30] A. Megretski, “Global stability of oscillations induced by a relay feedback,” *IFAC Proceedings Volumes*, vol. 29, no. 1, pp. 1931 – 1936, 1996, 13th World Congress of IFAC, 1996, San Francisco USA, 30 June - 5 July. [Online]. Available: <http://www.sciencedirect.com/science/article/pii/S1474667017579537>

[31] P.-A. Bliman and A. Krasnosel’skii, “Periodic solutions of linear systems coupled with relay,” *Nonlinear Analysis: Theory, Methods & Applications*, vol. 30, no. 2, pp. 687 – 696, 1997, proceedings of the Second World Congress of Nonlinear Analysts. [Online]. Available: <http://www.sciencedirect.com/science/article/pii/S0362546X96003720>

- [32] S. Varigonda and T. T. Georgiou, "Dynamics of relay relaxation oscillators," *IEEE Transactions on Automatic Control*, vol. 46, no. 1, pp. 65–77, Jan 2001.
- [33] K. H. Johansson and A. Rantzer, "Global analysis of third-order relay feedback systems," *IFAC Proceedings Volumes*, vol. 29, no. 1, pp. 1937–1942, 1996, 13th World Congress of IFAC, 1996, San Francisco USA, 30 June - 5 July. [Online]. Available: <http://www.sciencedirect.com/science/article/pii/S1474667017579549>
- [34] D. J. Allwright, "Harmonic balance and the Hopf bifurcation," *Math. Proc. Cambridge Philos. Soc.*, vol. 82, no. 3, pp. 453–467, 1977. [Online]. Available: <https://doi.org/10.1017/S0305004100054128>
- [35] G.-B. Stan and R. Sepulchre, "Analysis of interconnected oscillators by dissipativity theory," *IEEE Transactions on Automatic Control*, vol. 52, no. 2, pp. 256–270, 2007.
- [36] X. Ge, M. Arcak, and K. N. Salama, "Nonlinear analysis of ring oscillator and cross-coupled oscillator circuits," *Dyn. Contin. Discrete Impuls. Syst. Ser. B Appl. Algorithms*, vol. 17, no. 6, pp. 959–977, 2010.
- [37] J. C. Alexander and J. A. Yorke, "Global bifurcations of periodic orbits," *Amer. J. Math.*, vol. 100, no. 2, pp. 263–292, 1978. [Online]. Available: <https://doi.org/10.2307/2373851>
- [38] R. Balasubramanian, "Stability of limit cycles in feedback systems containing a relay," *IEE Proceedings D (Control Theory and Applications)*, vol. 128, pp. 24–29(5), January 1981. [Online]. Available: <https://digital-library.theiet.org/content/journals/10.1049/ip-d.1981.0005>
- [39] S. Majhi and D. Atherton, "Stability of limit cycles in relay control systems," *IFAC Proceedings Volumes*, vol. 31, no. 17, pp. 91–96, 1998, 4th IFAC Symposium on Nonlinear Control Systems Design 1998 (NOLCOS'98), Enschede, The Netherlands, 1-3 July. [Online]. Available: <https://www.sciencedirect.com/science/article/pii/S1474667017403168>
- [40] K. H. Johansson, A. Rantzer, and K. J. Åström, "Fast switches in relay feedback systems," *Automatica*, vol. 35, no. 4, pp. 539–552, 1999. [Online]. Available: <https://www.sciencedirect.com/science/article/pii/S0005109898001605>
- [41] S. G. Krantz and H. R. Parks, *The implicit function theorem*. Birkhäuser Boston, Inc., Boston, MA, 2002, history, theory, and applications. [Online]. Available: <https://doi.org/10.1007/978-1-4612-0059-8>
- [42] V. I. Arnol'd, *Ordinary differential equations*, 3rd ed. Berlin: Springer-Verlag, 1992.
- [43] C. A. Desoer and M. Vidyasagar, *Feedback systems*, ser. Classics in Applied Mathematics. Society for Industrial and Applied Mathematics (SIAM), Philadelphia, PA, 2009, vol. 55, input-output properties, Reprint of the 1975 original [MR0490289]. [Online]. Available: <https://doi.org/10.1137/1.9780898719055.ch1>
- [44] M.-H. Shih and J.-W. Wu, "Asymptotic stability in the Schauder fixed point theorem," *Studia Mathematica*, vol. 131, no. 2, pp. 143–148, 1998. [Online]. Available: <http://matwbn.icm.edu.pl/ksiazki/sm/sm131/sm13124.pdf>
- [45] M. Vidyasagar, "On undershoot and nonminimum phase zeros," *IEEE Transactions on Automatic Control*, vol. 31, no. 5, pp. 440–440, May 1986.
- [46] —, "Author's reply," *IEEE Transactions on Automatic Control*, vol. 32, no. 3, pp. 272–272, March 1987.
- [47] M. C. Irwin, *Smooth dynamical systems*, World Scientific Publishing Co., Inc., River Edge, NJ, 2001, vol. 17, reprint of the 1980 original, With a foreword by R. S. MacKay. [Online]. Available: <https://doi.org/10.1142/9789812810120>
- [48] E. A. Coddington and N. Levinson, *Theory of ordinary differential equations*. McGraw-Hill Book Co., Inc., New York-Toronto-London, 1955.
- [49] J. L. Willems, "The stability of oscillations in nonlinear networks," *IEEE Transactions on Circuit Theory*, vol. 15, no. 3, pp. 284–286, 1968.
- [50] V. Khatskevich and D. Shoiykhet, *Differentiable operators and nonlinear equations*, ser. Operator Theory: Advances and Applications. Birkhäuser Verlag, Basel, 1994, vol. 66. [Online]. Available: <https://doi.org/10.1007/978-3-0348-8512-6>
- [51] "Weierstrass function," Apr 2021. [Online]. Available: [https://en.wikipedia.org/wiki/Weierstrass\\_function](https://en.wikipedia.org/wiki/Weierstrass_function)
- [52] S. G. Krantz, "On limits of sequences of holomorphic functions," *The Rocky Mountain Journal of Mathematics*, vol. 43, no. 1, pp. 273–283, 2013. [Online]. Available: <https://doi.org/10.1216/RMJ-2013-43-1-273>
- [53] J. M. Maciejowski, "Right-half plane zeros are not necessary for inverse response," in *2018 European Control Conference (ECC)*, 2018, pp. 2488–2492. [Online]. Available: <https://doi.org/10.4064/sm-131-2-143-148>